UNCLASSIFIED

CENTRAL RESEARCH LIBRARY
DOCUMENT COLLECTION

MARTIN MARIETTA ENERGY SYSTEMS LIBRARIES
3 4456 0350290 2

ORNL-2158
Instruments
TID 4500 (13th ed.) cy. 4

POCKET ION CHAMBERS FOR BETA RADIATION DOSE

Harry H. Hubbell, Jr.
Robert D. Birkhoff
Raymond M. Johnson

CENTRAL RESEARCH LIBRARY
DOCUMENT COLLECTION

LIBRARY LOAN COPY

DO NOT TRANSFER TO ANOTHER PERSON

If you wish someone else to see this document, send in name with document and the library will arrange a loan.

OAK RIDGE NATIONAL LABORATORY
OPERATED BY
UNION CARBIDE NUCLEAR COMPANY
A Division of Union Carbide and Carbon Corporation
UCC
POST OFFICE BOX X · OAK RIDGE, TENNESSEE

UNCLASSIFIED

Printed in USA. Price 55 cents. Available from the

Office of Technical Services
U. S. Department of Commerce
Washington 25, D. C.

LEGAL NOTICE

This report was prepared as an account of Government sponsored work. Neither the United States, nor the Commission, nor any person acting on behalf of the Commission:

A. Makes any warranty or representation, express or implied, with respect to the accuracy, completeness, or usefulness of the information contained in this report, or that the use of any information, apparatus, method, or process disclosed in this report may not infringe privately owned rights; or

B. Assumes any liabilities with respect to the use of, or for damages resulting from the use of any information, apparatus, method, or process disclosed in this report.

As used in the above, "person acting on behalf of the Commission" includes any employee or contractor of the Commission to the extent that such employee or contractor prepares, handles or distributes, or provides access to, any information pursuant to his employment or contract with the Commission.

Unclassified ORNL-2158

Contract No. W-7405-eng-26

HEALTH PHYSICS DIVISION

POCKET ION CHAMBERS FOR BETA RADIATION DOSE

Harry H. Hubbell, Jr.
Robert D. Birkhoff
Raymond M. Johnson

Date Issued

APR 26 1957

Oak Ridge National Laboratory
Operated by
Union Carbide Nuclear Company
A Division of Union Carbide and Carbon Corporation
Post Office Box X
Oak Ridge, Tennessee

Unclassified

MARTIN MARIETTA ENERGY SYSTEMS LIBRARIES

3 4456 0350290 2

INTERNAL DISTRIBUTION

1. C. E. Center
2. Biology Library
3. Health Physics Library
4-6. Central Research Library
7. Reactor Experimental Engineering Library
8-24. Laboratory Records Department
25. Laboratory Records, ORNL R.C.
26. L. B. Emlet (K-25)
27. J. P. Murray (Y-12)
28. A. M. Weinberg
29. J. A. Swartout
30. E. D. Shipley
31. E. J. Murphy
32. M. L. Nelson
33. K. Z. Morgan
34. S. C. Lind
35. A. S. Householder
36. C. S. Harrill
37. C. E. Winters
38. A. H. Snell
39. E. H. Taylor
40. W. H. Jordan
41. T. A. Lincoln
42. A. Hollaender
43. F. L. Culler
44. D. W. Cardwell
45. E. M. King
46. M. T. Kelley
47-48. E. E. Anderson
49. R. S. Livingston
50. C. P. Keim
51. K. E. Cowser
52. C. D. Susano
53. L. B. Farabee
54. F. J. Davis
55. R. J. Morton
56. C. E. Haynes
57. Hugh F. Henry (K-25)
58. E. G. Struxness
59. W. E. Cohn
60-109. H. H. Hubbell
110. D. E. Arthur
111. J. Neufeld
112. D. D. Cowen
113. P. M. Reyling
114. H. A. Parker
115. M. J. Skinner
116. J. C. Hart
117. T. H. J. Burnett
118. W. J. Lacy
119. B. G. Saunders
120. G. S. Hurst
121. T. E. Bortner
122. J. A. Lane
123. R. W. Johnson
124. H. P. Yockey
125. C. E. Clifford
126. J. L. Gabbard
127. R. A. Charpie
128. G. E. Boyd
129. S. J. Cromer
130. L. C. Emerson (Y-12)
131. D. M. Davis
132. P. E. Brown
133. E. D. Gupton
134. J. C. Ledbetter
135. R. L. Clark
136. G. C. Cain
137. L. C. Johnson
138. W. Ogg
139. O. D. Teague
140. E. L. Sharp
141. E. J. Kuna
142. H. H. Abee
143. C. R. Guinn
144. A. D. Warden
145. S. R. Bernard
146. C. C. Sartain
147. J. R. Muir
148. J. A. Auxier
149. M. F. Fair
150. S. I. Auerbach
151. G. W. Royster, Jr.
152. R. R. Dickison
153. ORNL - Y-12 Technical Library, Document Reference Section
154. R. E. Yoder
155. F. W. Sanders
156. F. C. Maienschein
157. W. J. Boegly, Jr.
158. F. L. Parker

159. W. E. Lotz
160. B. Fish
161. M. B. Edwards
162. F. M. Empson
163. G. G. Robeck
164. R. D. Birkhoff
165. R. H. Ritchie
166. J. A. Harter
167. W. G. Stone
168. J. S. Cheka
169. P. N. Hensley
170. R. W. Peelle

EXTERNAL DISTRIBUTION

171. C. P. Straub, Public Health Service, Robert A. Taft Sanitary Eng. Center
172. R. M. Collier, University of Florida
173. Physics and Engineering Group, Balcones Research Center, RFD 4, Box 189, Austin, Texas
174. R. F. Bacher, California Institute of Technology
175. G. E. Thoma, USAF
176. H. J. McAlduff, AEC, Oak Ridge
177. Vanderbilt University, Physics Department Library
178. Vanderbilt University, Joint University Library
179. Massachusetts Institute of Technology, Department of Electrical Engr.
180. University of California, Gerhard Klein
181. R. M. Richardson, U.S. Geological Survey, 2-C P.O. Building, Knoxville, Tennessee
182. C. V. Theis, U.S. Geological Survey, Box 433, Albuquerque, New Mexico
183. Lola Lyons, Librarian, Olin Industries, Inc., East Alton, Illinois
184. Jack Story, University of Chicago, Argonne Cancer Research Hospital, 950 East 59th Street, Chicago 37, Illinois
185. J. H. Ebersole, USSS Nautilus, c/o Fleet Post Office, New York, New York
186. David Smith, Electric Boat Division, Groton, Connecticut
187. Division of Research and Development, AEC, ORO
188. S. C. Sigoloff, USAF, The Radiobiological Laboratory, University of Texas and U.S. Air Force, Austin, Texas
189. Robert Wood, Department of Physics, Memorial Center, 444 E. 68th Street, New York 21, New York
190. F. N. Huffman, Glenn L. Martin Co., Baltimore, Maryland
191. R. Schwaar, Chem. Engr. Lab., Princeton University, Princeton, New Jersey
192. L. V. Spencer, National Bureau of Standards, Washington 25, D.C.
193. H. H. Rossi, Columbia University, 630 W. 168th St., New York 32, New York
194. F. H. Attix, National Bureau of Standards, Washington 25, D. C.
195. Duane Mayhew, Victoreen Instrument Co., 5806 Hough Ave., Cleveland 3, Ohio
196. J. S. Laughlin, Memorial Center, 444 E. 68th Street, New York 21, New York
197. M. Danzker, Memorial Center, 444 E. 68th Street, New York 21, New York
198. Gail D. Adams, Jr., Radiological Lab., University of California, San Francisco 22, California

199-223. R. M. Johnson, Westinghouse Research Labs., Beulah Road, E. Pittsburgh, Pennsylvania

224-784. Given distribution as shown in TID 4500 (13th ed.) under Instruments category (100 copies - OTS)

TABLE OF CONTENTS

		Page
I.	Introduction	1
II.	Theory	5
	1. Average Energy of Electrons in a Water Solution of a Radioisotope	5
	2. Expected Dose Rate in an Air Cavity in a Water Solution of a Beta-Ray Emitter	18
	3. Method of Calculating Dose Rate in a Cavity from Observed Ionization	23
III.	Apparatus	24
	1. The Beta Calibration Cell	24
	2. The Pocket Ionization Chambers	29
	3. Apparatus for Measuring Gamma and X-Ray Response of Pencils	38
	4. Isotopes Used	44
	5. Plating Problems	46
IV.	Experimental Results	53
	1. Beta-Ray Calibration of Pocket Chambers	53
	2. Gamma and X-Ray Response of Pocket Chambers	61
	3. Errors and Estimated Accuracy	66
V.	Discussion	68
VI.	Conclusions	73
	Appendix	75
	1. Sample Calculation of Electron Flux in Water Solution	75
	2. Typical Data	88
	3. Summary of Beta Dosimeter Data	91
	4. Beta Dosimeter Responses as Percentages of Various Reference Values	92
	Bibliography	93

LIST OF TABLES

		Page
I.	Standard Filter Combinations and Kilovoltages	39
II.	Average Energies of Isotopes	45
III.	Assay Information and Error	50
IV.	Calculation of Electron Flux in Water for W^{185}	79

LIST OF FIGURES

		Page
1.	S^{35} Spectra	11
2.	Ca^{45} Spectra	12
3.	W^{185} Spectra	13
4.	Tl^{204} Spectra	14
5.	Ag^{111} Spectra	15
6.	P^{32} Spectra	16
7.	Y^{90} Spectra	17
8.	Beta Calibration Cell and Mylar Ionization Chamber Conversion	25
9.	Electrometer Circuit for Mylar Ion Chamber	27
10.	Plateau of Mylar Ion Chamber in P^{32} Solution	28
11.	Pocket Ionization Chambers	30
12.	Victoreen Pocket Meter, Model 362	31
13.	Drilled Plastic Wall Pocket Chamber	32
14.	Aluminum or Magnesium Wall Pocket Chamber	33
15.	Voltage Calibration and Scale Linearity in Minometer 287-1742	35
16.	Standard Free Air Chamber Diagram	41
17.	X-Ray Exposure Arrangement	43
18.	Response of Chambers Compared to that Calculated	54
19.	Response of Chambers Compared to Measured Ionization in Cavity	57
20.	Response of Chambers Compared to Paper Wall Chamber	59
21.	Gamma-Ray Reponse of Chambers I	62

List of Figures continued

Page

22. Gamma-Ray Response of Chambers II 63

23. Electrode Coating Effect on Gamma Response of Victoreen Chamber 64

24. Electrode Coating Effect on Gamma Response of Drilled Al Chamber 65

25. H(T) 82

26. Stopping Power in Water $S_Z(T)$ 83

27. Integrated Spectrum of W^{185} 84

ACKNOWLEDGMENTS

The authors wish to express their appreciation to L. B. Farabee, B. H. Ketelle and B. Kahn for assistance with the chemical problems; to R. H. Ritchie and J. S. Cheka for help on the calculations; and to H. A. Parker and his group for making the radio-assays of the solutions.

The method of calibrating the dosimeters by immersing them in a water solution was suggested to us by Dr. Harald H. Rossi, to whom grateful acknowledgment is made.

One of us (RMJ) held a Radiological Physics Fellowship of the U. S. Atomic Energy Commission during this work.

ABSTRACT

A pocket ionization chamber has been developed which in conjunction with a commercial gamma reading pocket chamber can be used to estimate the beta dose received, or if used alone, to measure the combined beta-gamma dose. The problem was to obtain a simple, rugged chamber which would have a wall sufficiently thin to pass the lower energy beta rays and which would give either no response for gamma rays or one of the same magnitude as the gamma reading pocket meter. Of the six dosimeters constructed and tested, the perforated aluminum walled chamber gave the best beta response. Its response over the range of average energies from about 52 kev to 694 kev varied from about 50% to about 80% of the dose received by the germinal layer of the skin. The response of this chamber to low energy gamma radiation (up to 700 kev) approximates that of the commercial Victoreen pocket chamber. All beta rays of energies less than that which will reach the basal layer of the epidermis were excluded by the 7 mg/cm^2 wall surrounding the sensitive volume. A new method is described for calibrating a pencil for a degraded spectrum of radiation, such as is commonly found in the field. The dosimeter is inserted into the center of an infinite homogeneous aqueous solution of a radioisotope whose beta ray spectrum is known. The dose rate measured by the various pencils is expressed as a percentage of the response of a 7 mg/cm^2 paper walled laboratory standard chamber; an effectively zero thickness wall Mylar ion chamber; or the dose rate as calculated from the Bragg-Gray principle and the specific activity of the solution. Included in this paper are the calculations of the flux of electrons in water solution for the beta emitters S^{35}, Ca^{45}, W^{185}, Tl^{204}, Ag^{111}, P^{32}, and Y^{90}.

I. INTRODUCTION

The health physicist has always concerned himself with the total beta plus gamma dose received by a person working in a radiation field. At ORNL this dose is estimated in advance by a surveyor using a "paper chamber Cutie Pie."[1] This instrument measures not only gamma radiation but beta radiation as well, while the pocket chamber worn by the worker in a radiation field measures essentially only the gamma radiation. As a result, there may be a large discrepancy between the dose estimated by the health physics surveyor and the dose that is read on the worker's pocket chamber. There is need therefore for a personnel dosimeter sensitive to beta rays.

The problems in attempting to build a beta-sensitive dosimeter are two fold—first, engineering problems in design, construction, and use, and, second, the problem of accurate calibration of such an instrument. The first problem was solved by the use of a pencil with a sensitive volume of the same size as that used in the standard gamma chambers. This volume is defined by a layer of conducting paper 7 mg/cm^2 thick, that being the

---

[1] This is an instrument in which an ion chamber with a minimum wall thickness of 7 mg/cm^2 is coupled with a balanced bridge circuit having an electrometer tube as one arm of the bridge. The ion current develops a voltage on the grid of the tube, unbalancing the bridge and allowing a current proportional to the ionization in the chamber to pass through a microammeter calibrated in mr/hr.

assumed minimum depth of the cells in the basal layer of the human epidermis.[2,3] Thus the radiation seen by the pencil is the same as is seen by the germinal layer of the skin. To give mechanical strength to this paper chamber an outer cylinder of perforated aluminum, magnesium or drilled plastic is slipped over the paper chamber. The overall size is the same as the standard pocket pencil, and since the sensitive volume is the same, it may be read with the same Minometer to approximately the same $\pm$ 10% accuracy[4] of reading.

The accurate calibration of the beta chamber involves securing a strong, known spectrum of beta radiation. One cannot get point or plane sources of sufficient activity to be useful which still emit an undistorted thin source spectrum. Due to the very short range of betas in a finite medium, the spectrum is degraded to an unknown extent. In addition, the range of betas in air is a limiting factor, being only 0.11 meter for 100 kev electrons and only 3.7 meters for a 1 Mev electron. Another obstacle to the use of the source in air is the lack of accurate knowledge of the coefficients of attenuation of betas in air. Attempts to calibrate the chambers in cylinders of natural uranium were not satisfactory because

---

[2] National Bureau of Standards, "Permissible Dose from External Sources of Ionizing Radiation," Handbook 59, p. 39, U. S. Department of Commerce, Washington, D. C. (September 1954).

[3] In commercial construction this paper might be replaced by a plastic wall coated inside with graphite and having the same superficial density of 7 mg/cm^2.

[4] Frank H. Day, "X-Ray Calibration of Radiation Survey Meters, Pocket Chambers, and Dosimeters," p. 6, NBS Circular 507.

of the difficulties encounted in calculating the electron flux spectrum in this material.

The calibration problem was solved by using a very thin walled cavity in a homogeneous water solution of a beta emitting isotope. The cell holding the solution was large in dimensions compared to the range of highest energy betas emitted. Hence it was possible to calculate the dose easily from a knowledge of the primary beta energy spectrum and the specific activity of the solution.

The theoretical problems which are considered in this report are then as follows:

1. The calculation of the average energy of the primary and secondary electrons in this cavity. This required the calculation of the spectra of these electrons for each isotope;

2. The method of calculating the expected dose rate in a cavity in water solution of a beta-emitting radioisotope from its beta spectrum and specific activity;

3. The method of determining experimentally the dose rate in the cavity from the observed ionization there. These dose rates served as checked on those calculated by method 1.

The experimental problems which are discussed are these:

1. The design of a reasonably strong pocket ionization chamber with thin walls;

2. The design of a calibration cell for these chambers which has a cavity with walls of negligible thickness surrounded by water solution;

3. The choice, handling and assay of the radioisotopes;

4. The comparison of the observed dose rates in water solutions of beta ray emitting isotopes with those calculated;

5. The effect of cavity wall thickness on the dose rate in a cavity in the solution;

6. The response of the pencil chambers to gamma and x rays;

7. The interpretation of the results on beta and gamma response of the chambers in terms of permissible exposures to personnel.

II. THEORY

1. Average Energy of Electrons in a Water Solution of a Radioisotope

All pencil response curves for beta radiation were obtained from isotopes in a water solution. Therefore, it was preferable that results be given as a function of the average energy of the beta flux in that medium rather than the maximum or average energy of the nuclear beta spectrum. A method of calculating the beta flux in a medium has been given recently by Spencer and Fano,[5] and reviewed recently by R. D. Birkhoff.[6]

In the theory the usual continuous slowing down approximation to the electron spectrum (in which the flux is given at any energy by the reciprocal stopping power) is modified by the inclusion of secondary electrons generated by the few violent collisions experienced by the primary electrons, and by the inclusion of the energy losses due to bremsstrahlung. The statistical balance of electrons of energy T is given by

$$y(T) \int_0^T k(T, \tau)d\tau = \int_0^\infty y(T + \tau)\, k(T + \tau, \tau)d\tau + N(T) \qquad (1)$$

---

[5] L. V. Spencer and U. Fano, "Energy Spectrum Resulting from Electron Slowing Down," Phys. Rev. 93, 1172 (1954).

[6] R. D. Birkhoff, "Passage of Fast Electrons Through Matter," Section G-29, HANDBUCH DER PHYSIK, Vol. 34, Berlin: Julius Springer, (to be published).

where $y(T)$ has the dimensions cm energy^{-1} and represents the distance covered by electrons of energy T per unit energy interval. (The function $y(T)$ may also be considered to represent the flux of electrons with dimensions of the number of electrons per cm^2 per sec per unit energy). The symbol $k(T, \tau)$ indicates the probability per unit path of an energy loss τ from an electron of energy T, and the $N(T)$ indicates the number of electrons being born at energy T from the beta-ray continuous spectrum. In principle the problem may now be solved as the function $k(T, \tau)$ is just the Möller[7] cross section. Stepwise numerical methods may be used starting at the higher energy T_0 and working down in energy. However, the unfortunate large increase in $k(T, \tau)$ as τ becomes very small renders such an approach unworkable. Recasting the problem in integral form, the equivalent of the above equation may be written,

$$\int_T^\infty dT' \; y(T') \; K(T', T) = \int_T^\infty N(T')dT' \tag{2}$$

where

$$K(T', T) = \int_{T'-T}^\infty k(T', \tau)d\tau \tag{3}$$

---

[7] C. Möller, Ann. d. Physik 14, 531 (1932).

and is the probability per unit path that an electron of energy T' drops below an energy T. The left side of the equation now states that all electrons of energy T or greater will drop below T somewhere, and the right side gives the number of such electrons. The integral cross section K(T', T) contributes excessively to the integral only for T' very near T. In order to simplify still further the integration over T' in this critical range, Spencer and Fano introduce a new function $\overline{K}(T', T)$, which is defined so as to be everywhere close to K(T', T). This method of attack allows the problem to be reformulated in terms of the function $\left[y(T') K(T', T) - y(T) \overline{K}(T', T) \right]$ and the solution then becomes

$$y(T) = \left[F(T_o, T)\right]^{-1} \left\{ \int_T^{T_o} N(T')dT' - \int_T^{T_o} dT' \left[y(T') K(T', T) - y(T) \overline{K}(T',T) \right] \right\} \tag{4}$$

with the first integral representing the first approximation to the flux spectrum, and the second integral the effect on the flux of bremsstrahlung and secondary electron production. The function $F(T_o, T)$ is given by

$$F(T_o, T) = \int_T^{T_o} dT\, \overline{K}(T', T) \quad . \tag{5}$$

In obtaining a solution to the above equation the electron-electron collisions are considered as being responsible for both a loss of energy from the primary flux and as a source of secondary electrons which contribute to the flux at lower energies. The bremsstrahlung losses are divided in such a way that the smaller losses are considered as dissipating energy from the primary radiation while the larger losses are treated as a negative source of electrons. The final integral equation, although somewhat involved algebraically, permits a straightforward numerical evaluation.

For moderate initial electron energies the bremsstrahlung may be neglected if absorption takes place in a light material. Under these conditions the theory may be approximated by the simple expression,

$$y(T) = \left[S_Z(T)\right]^{-1} \left\{ \int_T^{T_o} N(T')dT' + \int_{2T}^{T_o} K_s(T', T)\, y(T')dT' \right\} \tag{6}$$

where $S_Z(T)$ is just the average stopping power at energy T; $N(T')$ is the source spectrum, and $K_s(T', T)$ may be taken as

$$K_s(T', T) = \frac{2\pi N_e r_o^{\,2}}{(\beta')^2} \left\{ T^{-1} - (T' - T)^{-1} \right\} \tag{7}$$

with N_e the electronic density in the medium and $r_o = e^2/m_o c^2$. The first

integral represents the contribution from the primary electrons, and the second integral is the buildup of secondaries.

Calculations with the above simplification have been carried out (see Appendix, SAMPLE CALCULATIONS, Part 1) for sources used in the experiment and the results are shown in Figs. 1 - 7. Although the stopping power and electron-electron scattering cross section (contained in K_s) are not well known at low energy, calculations were carried down to 1 kev. The results indicate a large buildup of electrons at low energy which may well be important biologically.

It is to be noted that N(T) and y(T) are physically and dimensionally different quantities and are plotted on the same coordinates in Figs. 1 - 7 for convenience only. The relative heights of points on the two curves at any energy are not comparable or significant because of normalization used. Only the general shapes of the curves are to be compared.

The average energy of the electrons in each of these spectra was calculated in the usual way as $\overline{T}_N$ from the equation

$$\overline{T} = \int_0^{T_o} T\, N(T)dT \Bigg/ \int_0^{T_o} N(T)dT \qquad (8)$$

and similarly for $\overline{T}_y$ for the flux y(T). The results are marked on the abscissae scales of the figures.

The value $\overline{T}_N$ was used in computing the average energy absorbed in

the water per unit volume. The value $\overline{T}_y$ was considered to measure the average energy of the flux of electrons traversing the water solution.

The energy loss for electrons in a small air cavity in the medium will be negligible, so the spectrum of electrons in the cavity is also y(T). Hence the abscissae of points on the response curves to be discussed below for our chambers were taken as the values of $\overline{T}_y$ from the y(T) spectra.

The values for $\overline{T}$ in each case depend on the shape of the spectrum of the betas emitted. For those elements whose spectra are well known we can assign the average energy within about $\pm$ 3%, but in several cases the spectra are not "allowed" spectra, and the accuracy of the experimental data available for these spectra does not justify an estimated limit of error smaller than $\pm$ 10%. The experiments referred to in some cases suffered from backscattering, thick sources, and absorption in the counter walls.

UNCLASSIFIED
ORNL-LR-DWG 15119

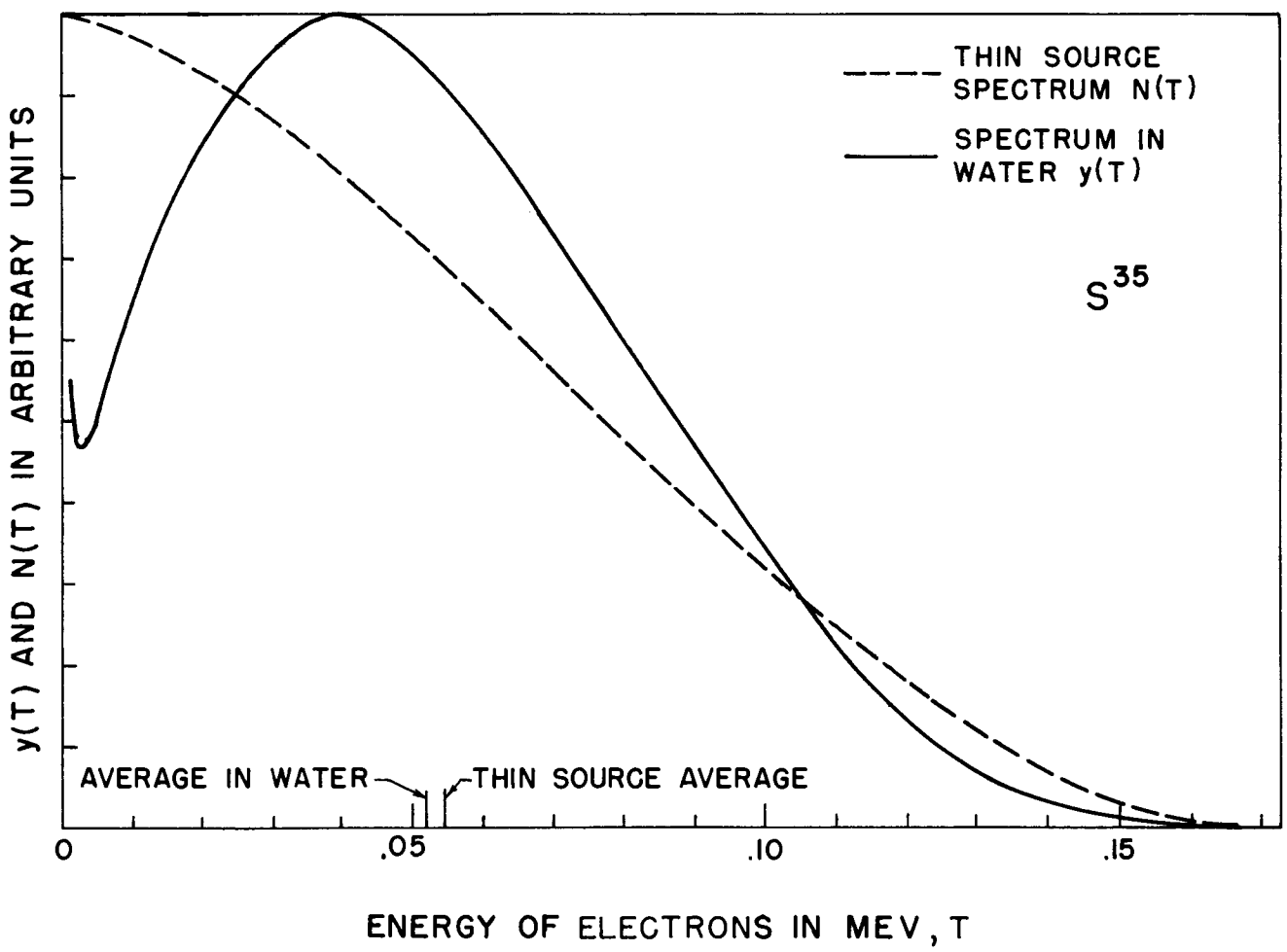

FIG. 1- S^{35} SPECTRA

UNCLASSIFIED
ORNL—LR—DWG 15121

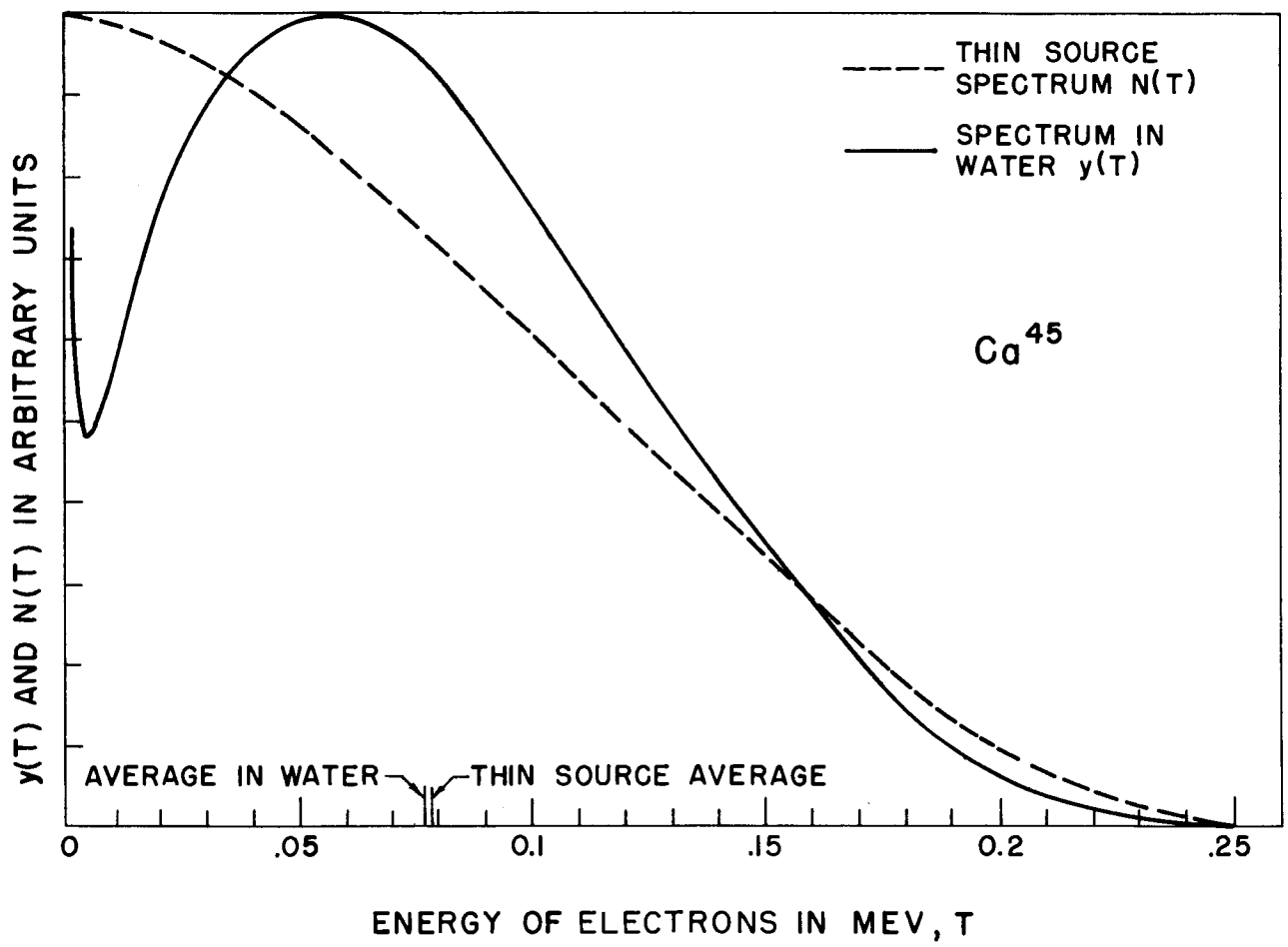

FIG. 2-Ca^{45} SPECTRA

UNCLASSIFIED
ORNL-LR-DWG 15118

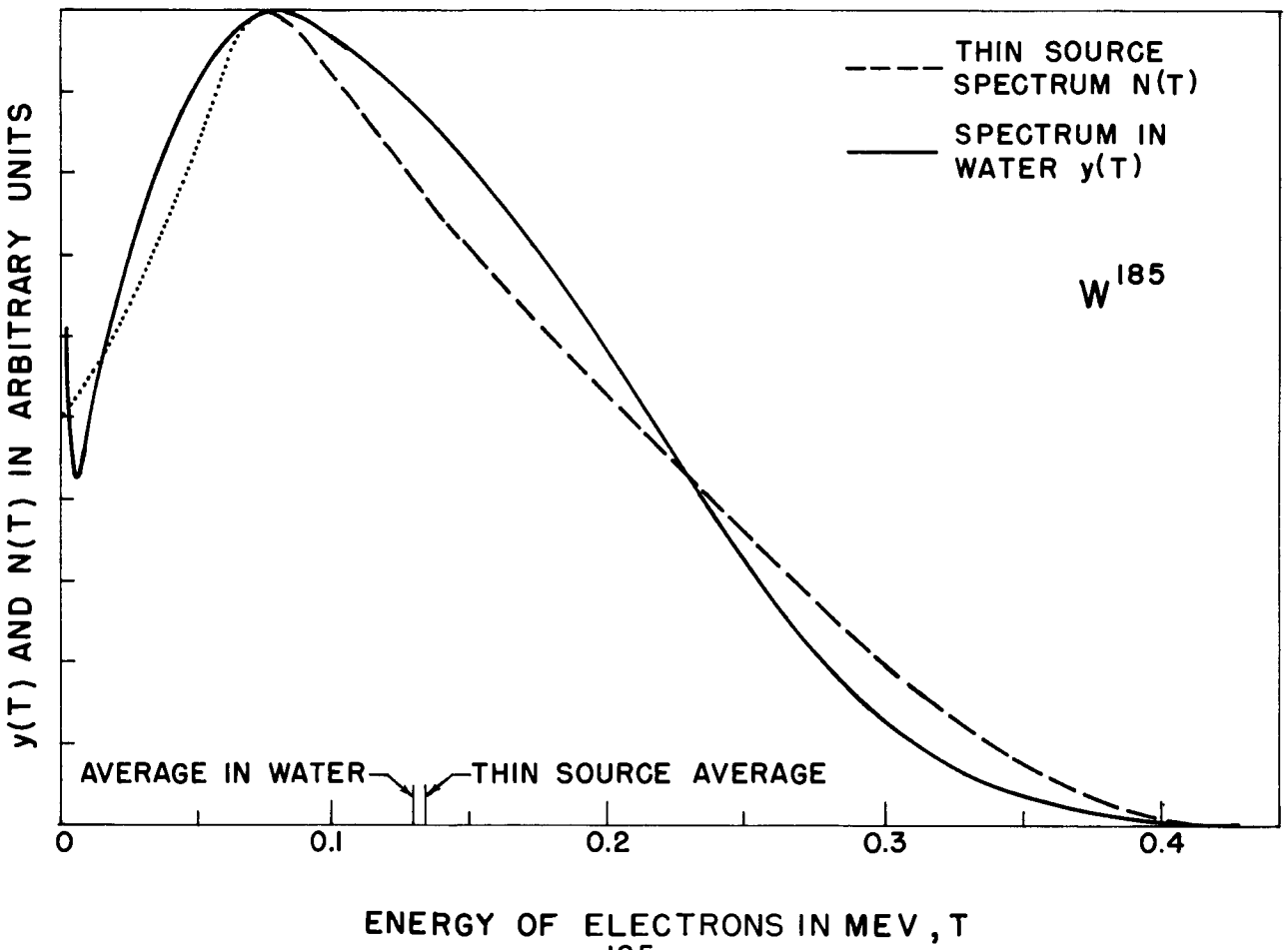

FIG. 3- W^{185} SPECTRA

UNCLASSIFIED
ORNL-LR-DWG 15123

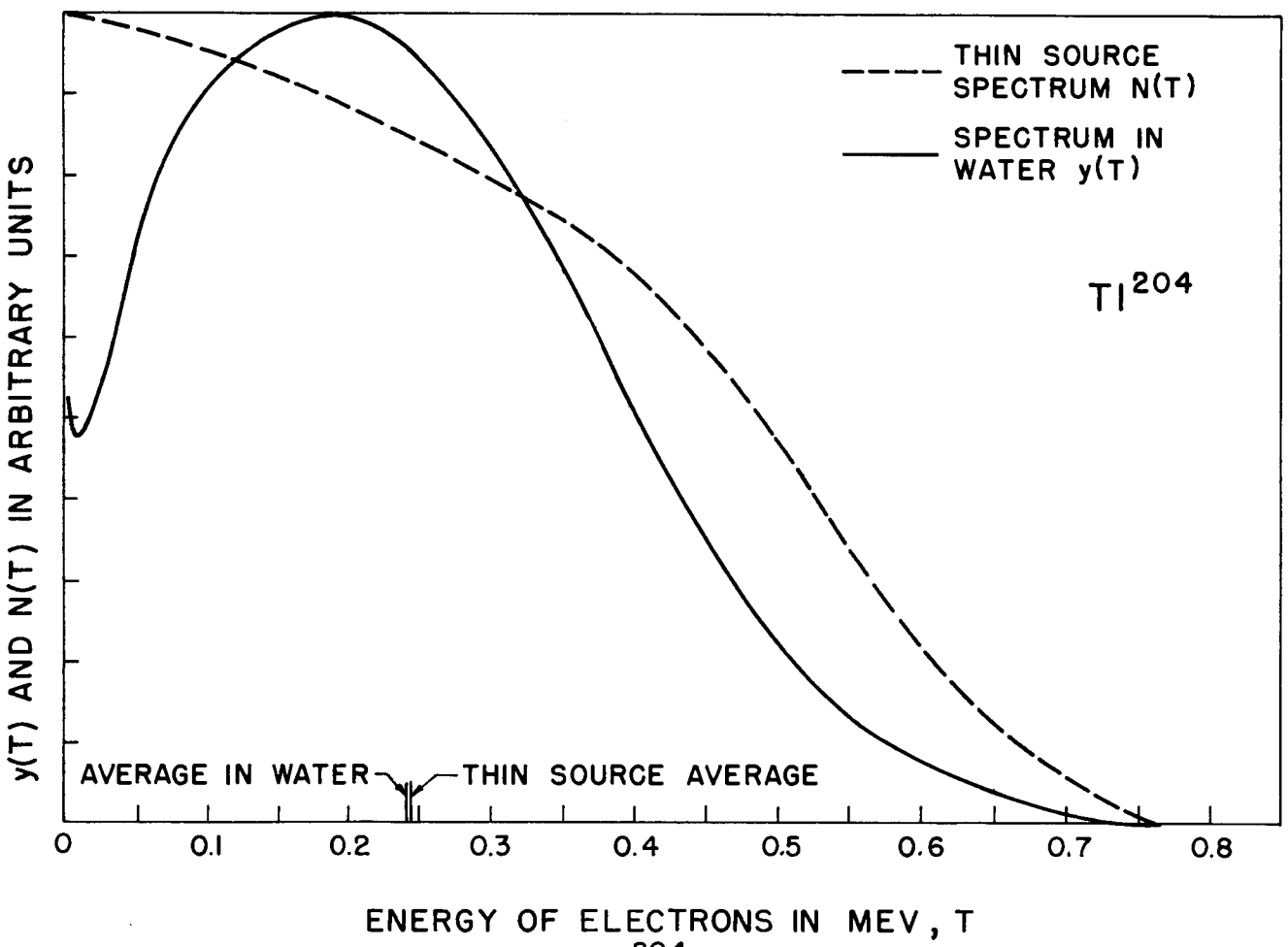

FIG. 4 - Tl^{204} SPECTRA

UNCLASSIFIED
ORNL—LR—DWG 15117

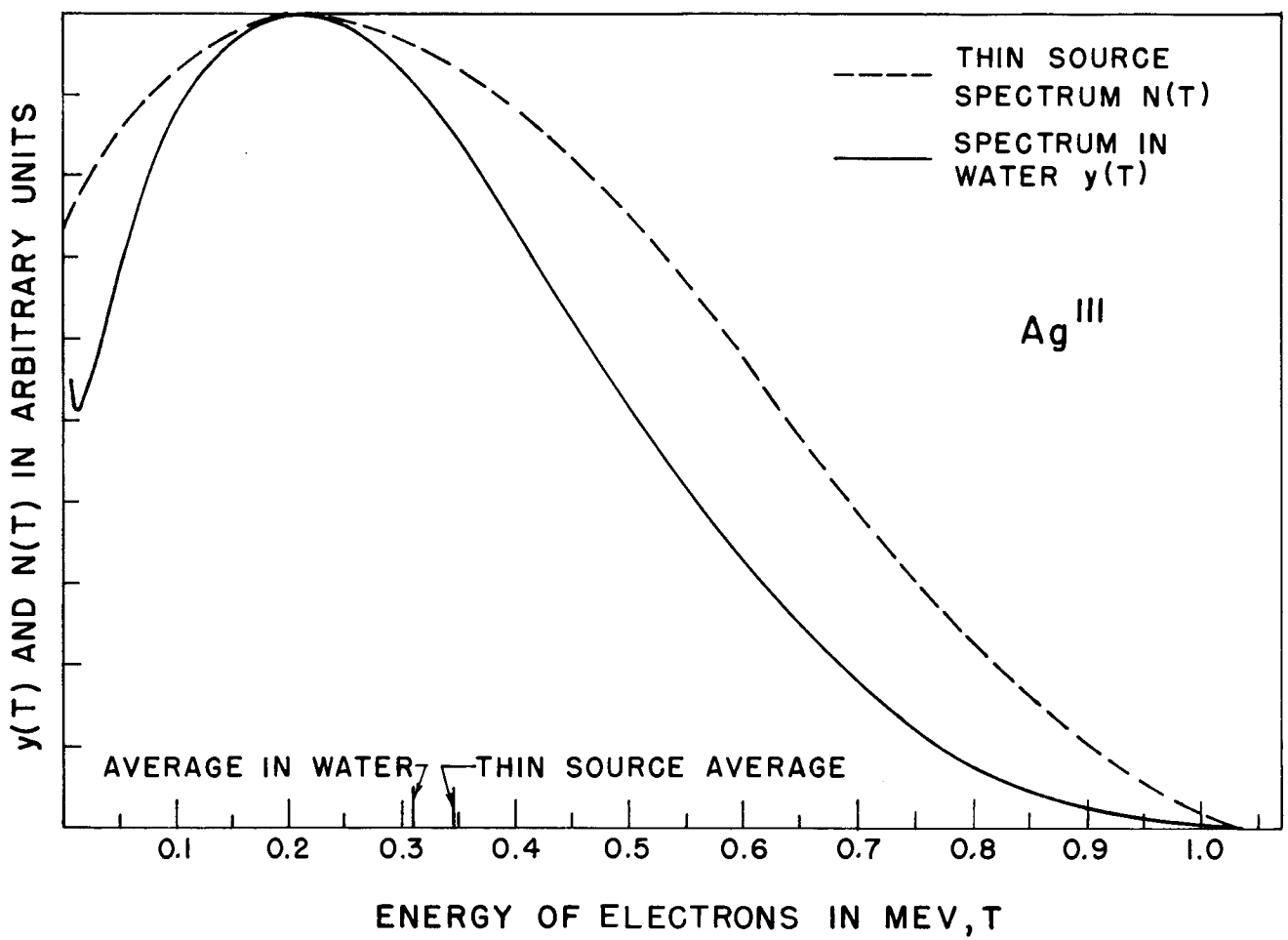

FIG. 5 - Ag^{111} SPECTRA

THIS DWG. SUPERSEDES 12562
UNCLASSIFIED
ORNL-LR-DWG 15122

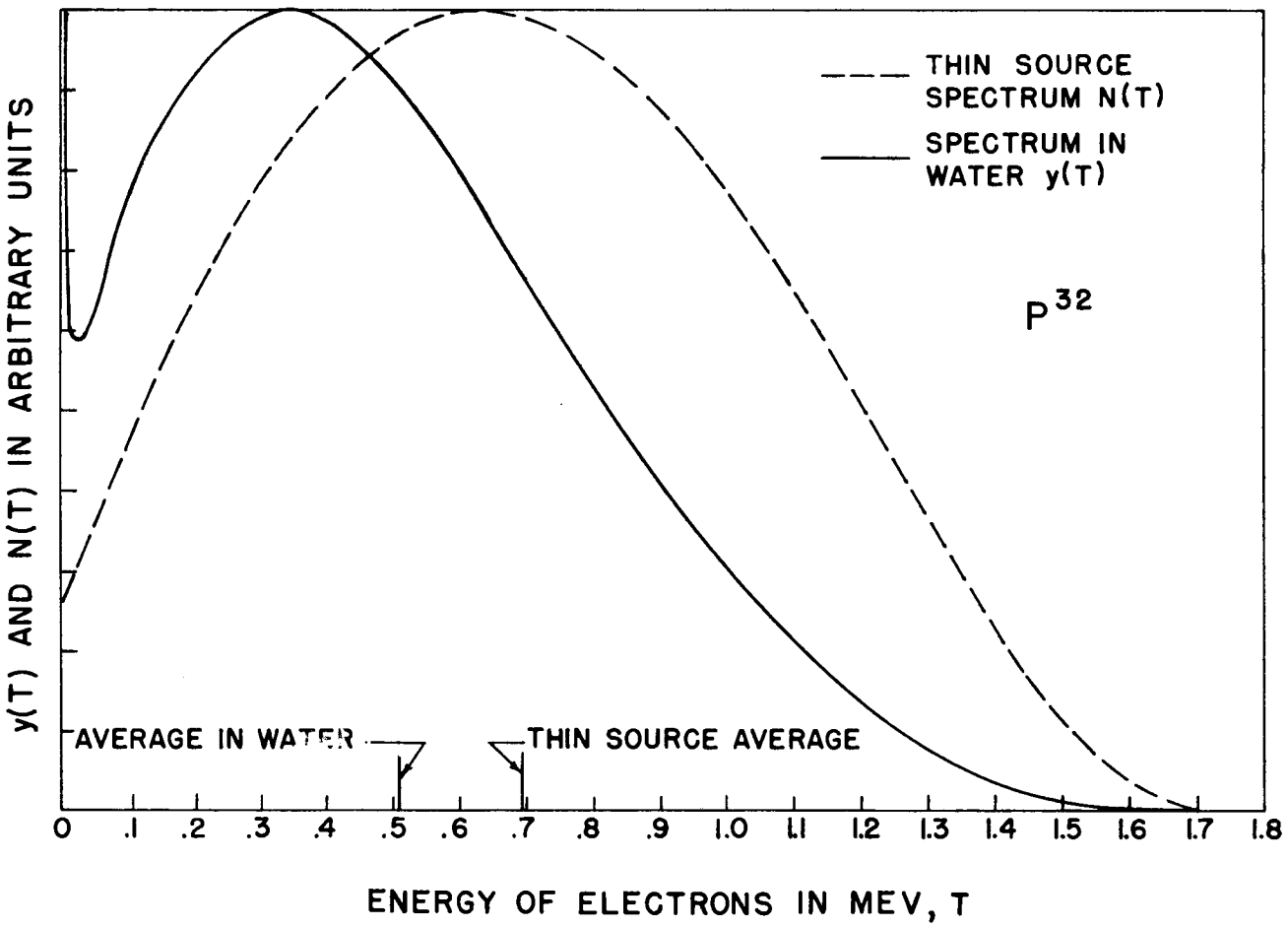

FIG. 6 - P^{32} SPECTRA

UNCLASSIFIED
ORNL-LR-DWG 15120

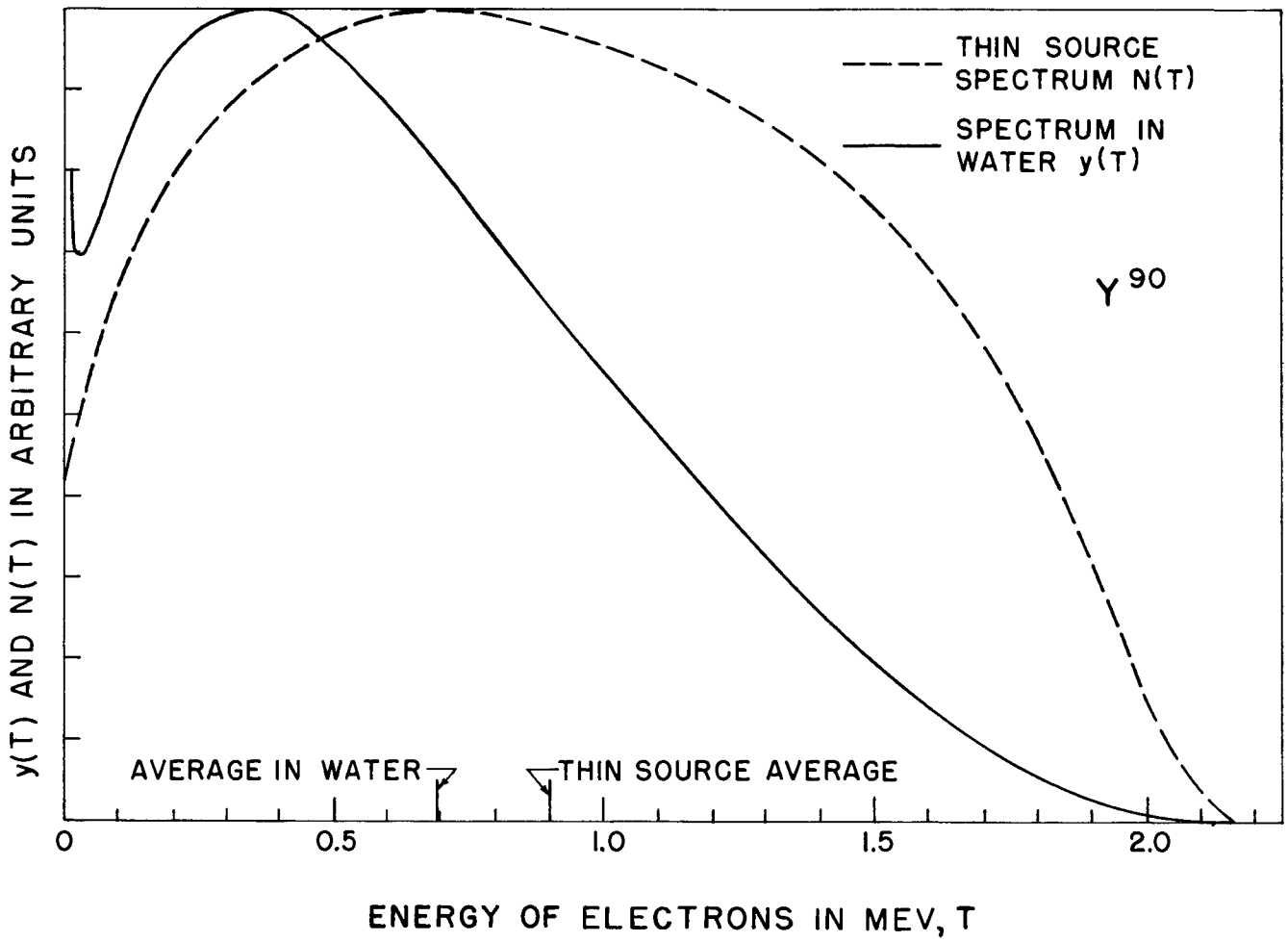

FIG. 7- Y^{90} SPECTRA

2. Expected Dose Rate in an Air Cavity in a Water Solution of a Beta-Ray Emitter

Consider the situation near the center of a water solution of a beta-ray emitting radioisotope contained in a vessel whose dimensions are large compared to the range in water of the most energetic beta ray present.[8] The amount of energy liberated per gram of solution per second must be the same as the amount of energy absorbed per gram of solution per second. The latter is the calculated dose rate in the water solution, D_w, in ev/(gm sec). If there are Q_m microcuries of radioactivity per gram of solution, the dose rate will be given by

$$D_w = 3.7 \times 10^4 \, Q_m b T_o \times 10^6 \tag{9}$$

and $b = \overline{T}_N / T_o$. (10)

The value, b, of the ratio of the average beta energy of the thin source spectrum, $\overline{T}_N$, in Mev, to the maximum energy of the thin source beta spectrum, T_o, in Mev, was obtained planimetrically from the ratio of the areas under the curves of the beta spectra, N(T), Figs. 1 - 7, divided into the areas under the curves obtained by multiplying the ordinates of the beta spectra at each energy by the value of the energy at that point, according to Eq. (8). This value obtained from the planimetric approach

---

[8] H. H. Rossi and R. H. Ellis, "Calculations for Distributed Sources of Beta Radiation," Am. J. Roent. and Ra. Therapy 67, 980 (1952).

may be approximated by an empirical equation given by K. Z. Morgan,[9]

$$b = \bar{T}/T_o = 0.33\ (1 - Z^{1/2}/50)(1 + T_o^{1/2}/4). \qquad (11)$$

As an example we take P^{32}. From Eq. (11) we get b = 0.404 as compared with a planimetric value of 0.409.

One then uses the Bragg-Gray principle[10] to calculate the dose in an air cavity in the solution. The principle states that the energy deposited per gram of air in a small cavity in an irradiated medium is equal to the energy deposited per gram in the medium, multiplied by the ratio of the stopping power per gram of air to that per gram of medium for the electrons traversing the cavity and medium. If the stopping power per electron is denoted by S_e, the energy deposited per cubic centimeter in the cavity is

$$D_a = D_w \frac{(S_e)_a\ (Z_a/A_a)\ N_o\ \rho_a}{(S_e)_w\ (Z_w/A_w)\ N_o\ \rho_w} \qquad (12)$$

---

[9] K. Z. Morgan, "Health Control and Nuclear Research," Chap. VI, Eq. 6-8, (to be published). K. Z. Morgan, "Handbook of Radiation Hygiene," Hanson Blatz, ed., Chap. 15, Eq. 11, (to be published by McGraw-Hill, N.Y.) An earlier form of this equation was included by Morgan as the second term in Eq. C5, p. 35, in Suppl. No. 6, Brit. J. Radiol. (London 1955), "Recommendations of the Int. Comm. on Radiological Protection."

[10] (a) W. Bragg, STUDIES IN RADIOACTIVITY, London, MacMillan and Co. (1912); (b) L. H. Gray, Proc. Roy. Soc. (Lond.) 122A, 647 (1929); (c) L. H. Gray, Proc. Roy. Soc. (Lond.) 156A, 578 (1936); (d) L. H. Gray, Brit. J. Radiol. 10, 600, 721 (1937); (e) L. H. Gray, Proc. Camb. Phil. Soc. 40, 72 (1944).

or $$D_a = (3.7 \times 10^4)\, Q_m b T_o \times 10^6 \frac{\rho_a}{\rho_w B_w} \tag{13}$$

where

$$B_w = \frac{(S_e)_w (Z_w/A_w)}{(S_e)_a (Z_a/A_a)} \quad . \tag{14}$$

B_w is the ratio of the mass stopping power of the medium to that of air and has values ranging from 1.025 at beta energy of 0.1 Mev to 1.019 at 1.0 Mev. The density ρ_a and ρ_w were taken to 0.001293 gm/cm^3 and 1.00 gm/cm^3 and thus the above dose rate is assumed to be at 0° C. and 760 mm Hg. N_o is Avogadro's number; Z and A are the atomic number and atomic weight.

The dose rate in the cavity may be expressed in "acres" per unit time, D_a', where the acre (air cavity roentgen equivalent) is defined as 1 esu/cm^3 at 0° C. and 760 mm Hg. Then[11]

$$D_a' = \frac{e}{W} D_a = \frac{4.80 \times 10^{-10}}{34.1} D_a \quad . \tag{15}$$

Substituting all the numerical values we get

$$D_a' = 0.660\, Q_m b T_o \tag{16}$$

---

[11] The value of W for air, 34.1 electron volts per ion pair, was averaged from Table I of W. P. Jesse and J. Sadauskis, Phys. Rev. 97, 1688 (1955).

where D_a' is in milliacres/sec; Q_m is in microcuries/ml; bT_o is the average beta energy in Mev released per disintegration.

Gray[12] found a lack of proportionality of ionization in his chamber to air pressure at low pressure which may now be understood in the light of the Spencer-Attix[13] theory and which explains the work of Attix and DeLaVergne[14] as well. The relation between the ionization in the cavity and the energy absorbed in the walls depends on two things, first, the constant value W, and second, B_w which is the energy dissipated in the cavity walls relative to that dissipated in the cavity gas. The Spencer-Attix theory deals primarily with the second factor. The Bragg-Gray theory is based on a simple schematization. Electrons are thought of as slowing down continuously by a sort of "friction" process as they travel through the medium, that is, the actual slowing down by a large number of collisions is approximated by a continuous energy loss. Energy is thought of as being dissipated only along the track at a rate given by the local stopping power. Therefore, secondary electrons generated along the track of the primaries by knock-on collisions are implicitly assumed to dissipate their energy at the spot where they are generated.

The Spencer-Attix formalism is a bit more complex. They consider

---

[12] L. H. Gray, op. cit. Ref. 10c.

[13] L. V. Spencer and F. H. Attix, "A Theory of Cavity Ionization," Radiation Research 3, 239 (1955).

[14] F. H. Attix and L. DeLaVergne, "Cavity Ionization as a Function of Wall Atomic Number," (to be published).

all collisions which result in an energy transfer of less than some arbitrary value of energy Δ as dissipating their energy on the spot. The Δ can be thought of as roughly the kinetic energy required by an electron to cross the cavity. They consider all collisions with net energy transfer greater than Δ as not dissipating any energy at all; that is, the resultant secondary electron is considered as a part of the incident spectrum. The differences between the Bragg-Gray and Spencer-Attix results are apparent only where the atomic numbers of cavity gas and walls differ considerably. In the case of the air and water used in this work, no differences would be expected.

3. Method of Calculating Dose Rate in a Cavity from Observed Ionization

An electrode was inserted in the cavity in the radioactive solution and sufficient voltage applied between the electrode and the wall of the cavity, which was conducting, to collect all the ions formed. This ion current gave another measurement of the dose rate in the cavity to compare with that calculated by method (2) above. The dose rate D_i in milliacres per second would be

$$D_i = 3 \times 10^9 \frac{I}{V} \frac{t}{273} \frac{760}{P} \times 10^3 \qquad (17)$$

where I is the current in amperes; V is the volume in cm^3 from which ions are collected; t is the absolute temperature; and P is the corrected barometric pressure in mm Hg.

III. APPARATUS

1. The Beta Calibration Cell

The basic piece of apparatus was the beta calibration cell which holds the radioactive solutions. The cell (see Fig. 8) was so designed that the distance from the center sensitive volume to any wall is greater than the range of the maximum energy beta ray from any of the isotopes used. This cell was fitted with a vacuum tight top so that a partial vacuum could be obtained to keep the very thin walled central volume a constant cylindrical shape. This vacuum was necessary because the volume must be accurately defined to allow one to calculate the dose rate in roentgens per second from the number of ion pairs per cubic centimeter of volume. The central volume was defined by a one milligram per square centimeter thick wall made of Mylar plastic coated on one side with aluminum, and on the other side with about 75 micrograms per square centimeter of gold. This plastic was obtained coated with aluminum on both sides. The aluminum was digested off one side by floating the plastic on the surface of a bath of saturated NaOH solution. The sheet was then applied to the inner surface of a cylindrical metal backing plate and a uniform layer of 75 micrograms per square centimeter of gold was evaporated onto the plastic in a vacuum chamber. The Mylar sheet was then fitted to the cell, with the gold side next to the solution, and fastened to the stainless steel defining sleeves with Plyobond 30" cement and baked for 30 minutes at 110° C. to assure leak tight adhesion. After a test with water to check for pin holes or leaks, the cell was attached to a storage bottle containing the radioactive solution.

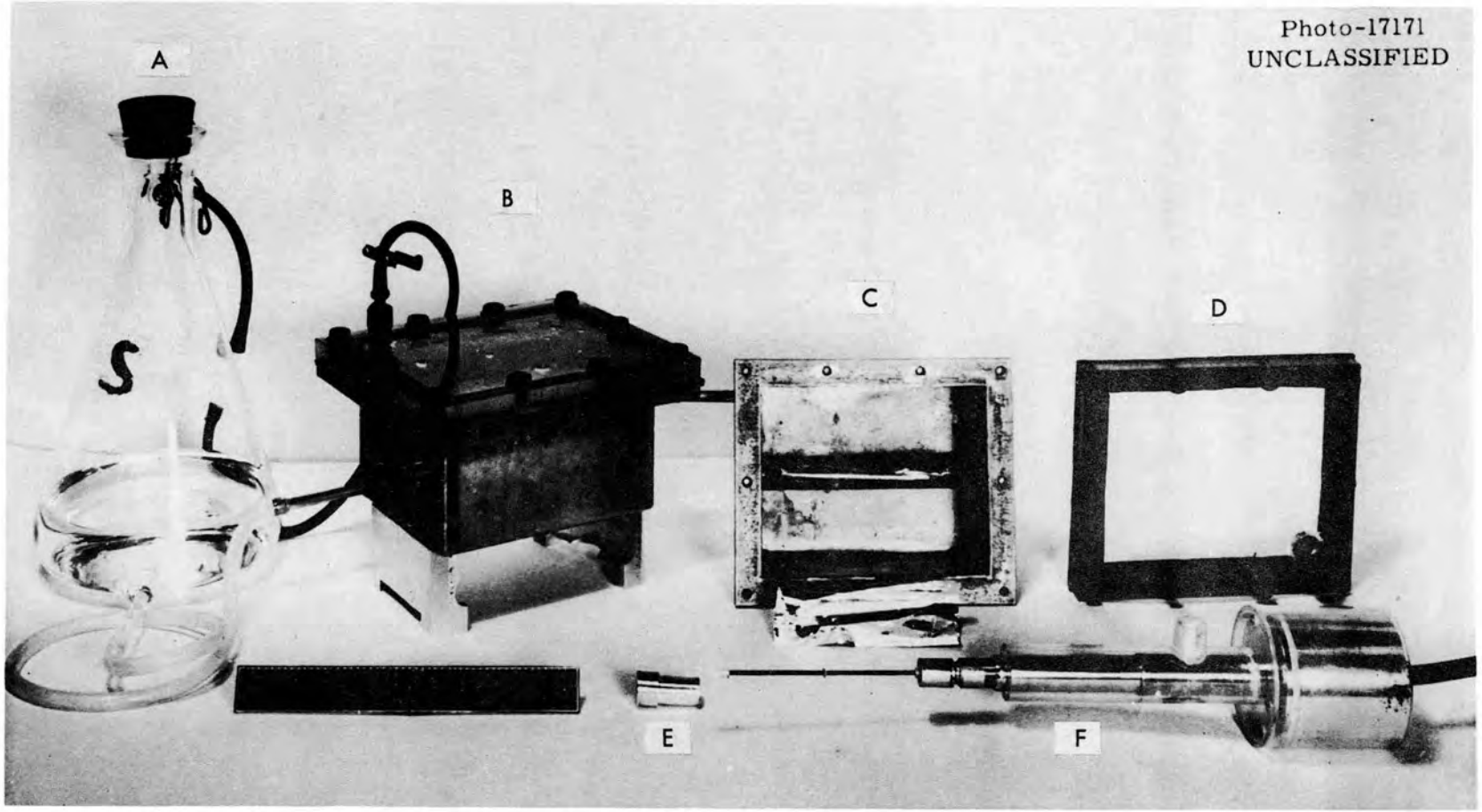

A. Solution Reservoir
B. Complete Cell
C. Cell Showing Center Mylar Chamber
D. Cover and Gasket
E. Volume Defining Plug
F. Center Electrode of Ion Chamber and Electrometer

FIG. 8. BETA CALIBRATION CELL AND MYLAR IONIZATION CONVERSION

Both the fluid inlet at the bottom and the air escape at the top were attached to the isotope storage bottle which was similarly equipped with top and bottom arms so that the whole system could be sealed from the air, thus preventing evaporation. The necessary partial vacuum was produced by sealing the top hose and lowering the storage bottle below the level of the cell. For timing the exposures in the cell, a Standard Electric Time Company timer, type S-60, was used.

To check the dose rate by the method discussed in Section II-3 an electrode from a Victoreen pocket ion chamber was placed in the center of the cavity to make it an ion chamber (Fig. 8) and the ends of the cavity were closed with aluminum plugs to define the volume. The ion current was measured by an electrometer (Fig. 9) used as a null instrument by bucking the voltage generated across a high resistor with a potentiometer. This ion chamber had an excellent plateau (Fig. 10).

UNCLASSIFIED
ORNL-LR-DWG. 19078

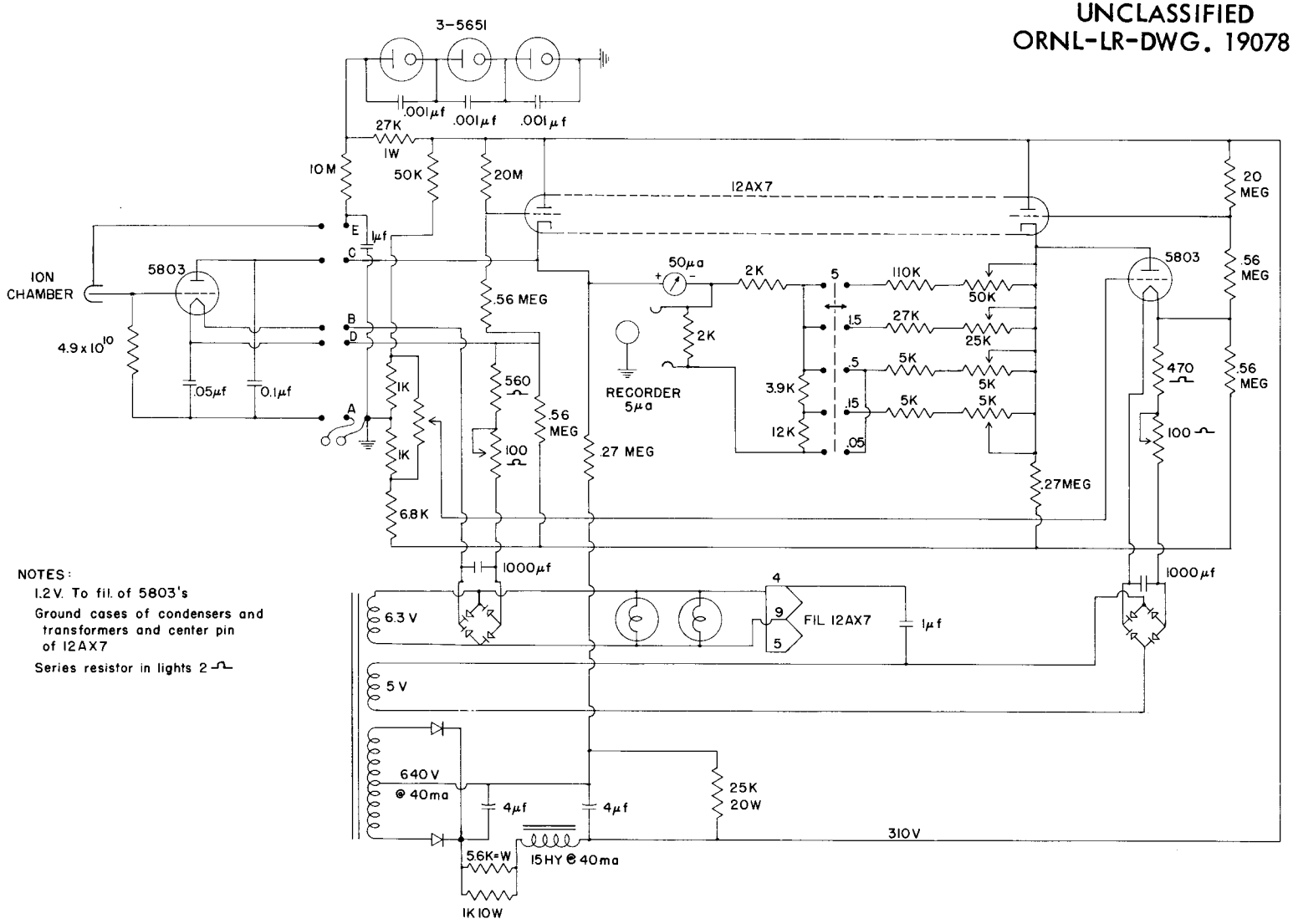

NOTES:
1.2V. To fil. of 5803's
Ground cases of condensers and transformers and center pin of 12AX7
Series resistor in lights 2 Ω

Fig. 9. Electrometer Circuit for Mylar Ion Chamber.

UNCLASSIFIED
ORNL-LR-DWG. 19079

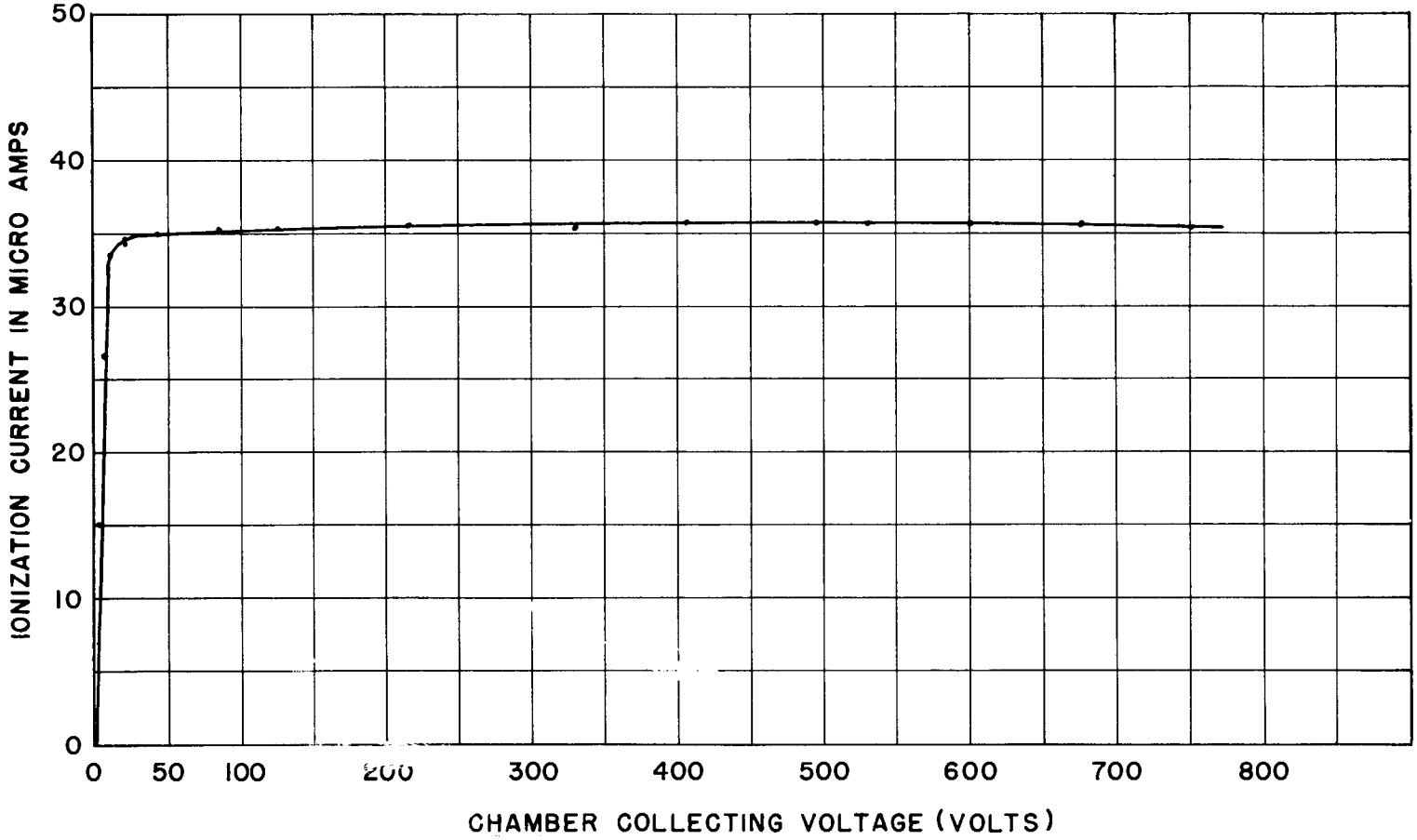

FIG. 10
PLATEAU OF MYLAR ION CHAMBER IN P32 SOLUTION

2. The Pocket Ionization Chambers

Seven types of pencils, shown in Fig. 11, were calibrated with beta, gamma, and x-rays. The general designs of these pencil chambers are shown in the accompanying figures.

Fig. 11. A. Victoreen pocket chamber model 362 (Fig. 12). A cutaway view and two types of center electrodes used are shown at H, Fig. 11.

B. The reference chamber made with a 7 mg/cm^2 conducting paper wall enclosing the same sensitive volume as (A).

C. A chamber made like (B) and surrounded by a 0.010" wall drilled aluminum tube (Fig. 14).

D. The Victoreen chamber modified by drilling away 40% of surface area and inserting a paper liner like (B) (Fig. 13).

E. A chamber like (C) but with the outer tube of magnesium (Fig. 14).

F. A chamber like (B) but surrounded by a stainless steel screen.

G. A chamber like (B) but surrounded by an aluminum screen.

The Victoreen chambers chosen were those which gave the Minometer fiber less than 2 mr kick when they were inserted or removed. The other chambers were treated to remove this "zero kick" by polishing the center electrode contact with emery cloth and treating them with a mild acid saline solution.

The central paper chamber volumes of all the pencils were made around the same mandril to insure the maximum possible uniformity of volume. Black conducting photographic paper of the proper weight was used and cut to size so that the overlap was as small as possible (approximately 1 mm). In manufacturing, the perforated walls could be stamped out of metal, or cast in plastic in a special die so that the

Photo-17172
UNCLASSIFIED

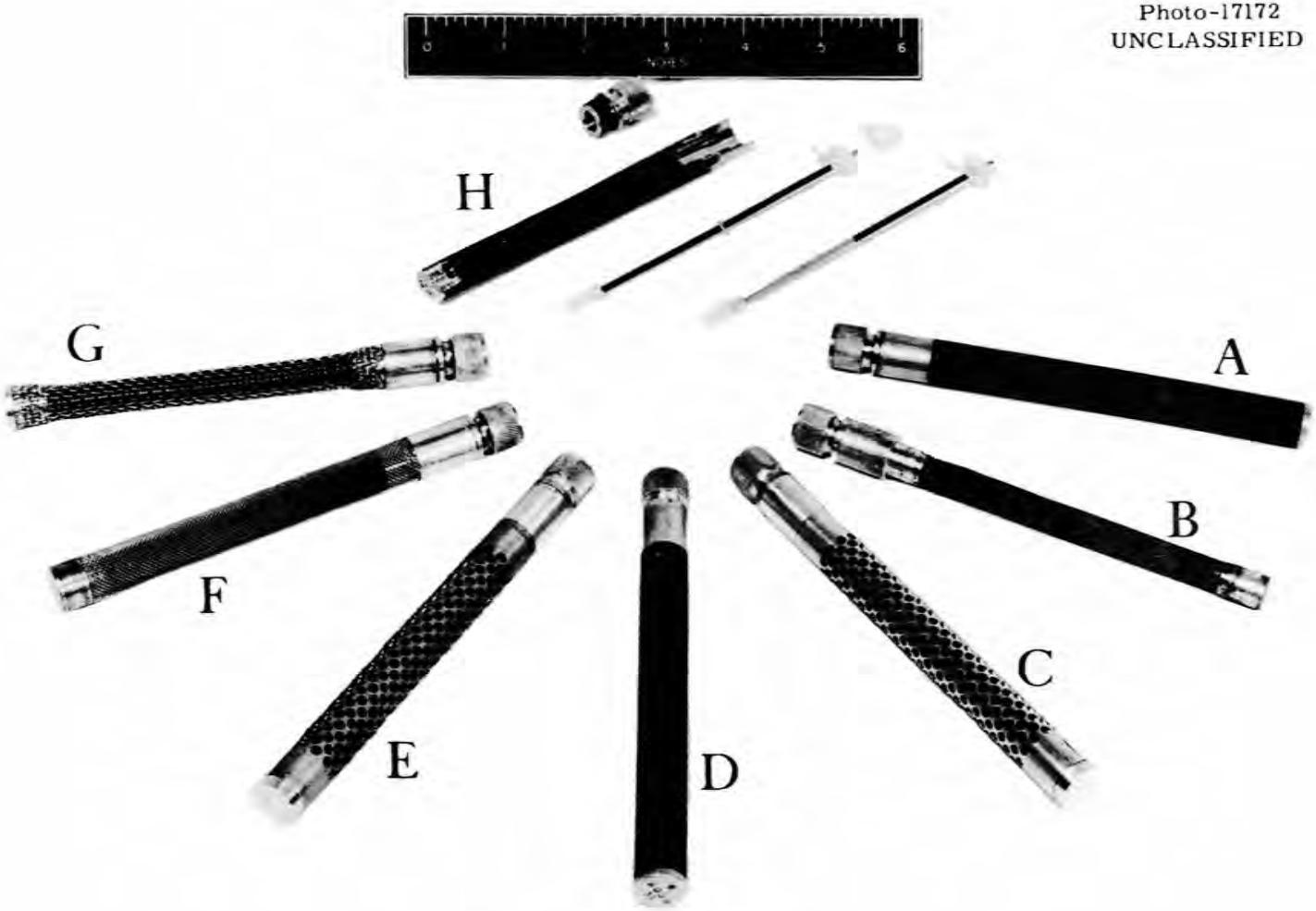

FIG. 11. POCKET IONIZATION CHAMBERS (SEE TEXT, P 29)

UNCLASSIFIED
ORNL-LR-DWG. 19080

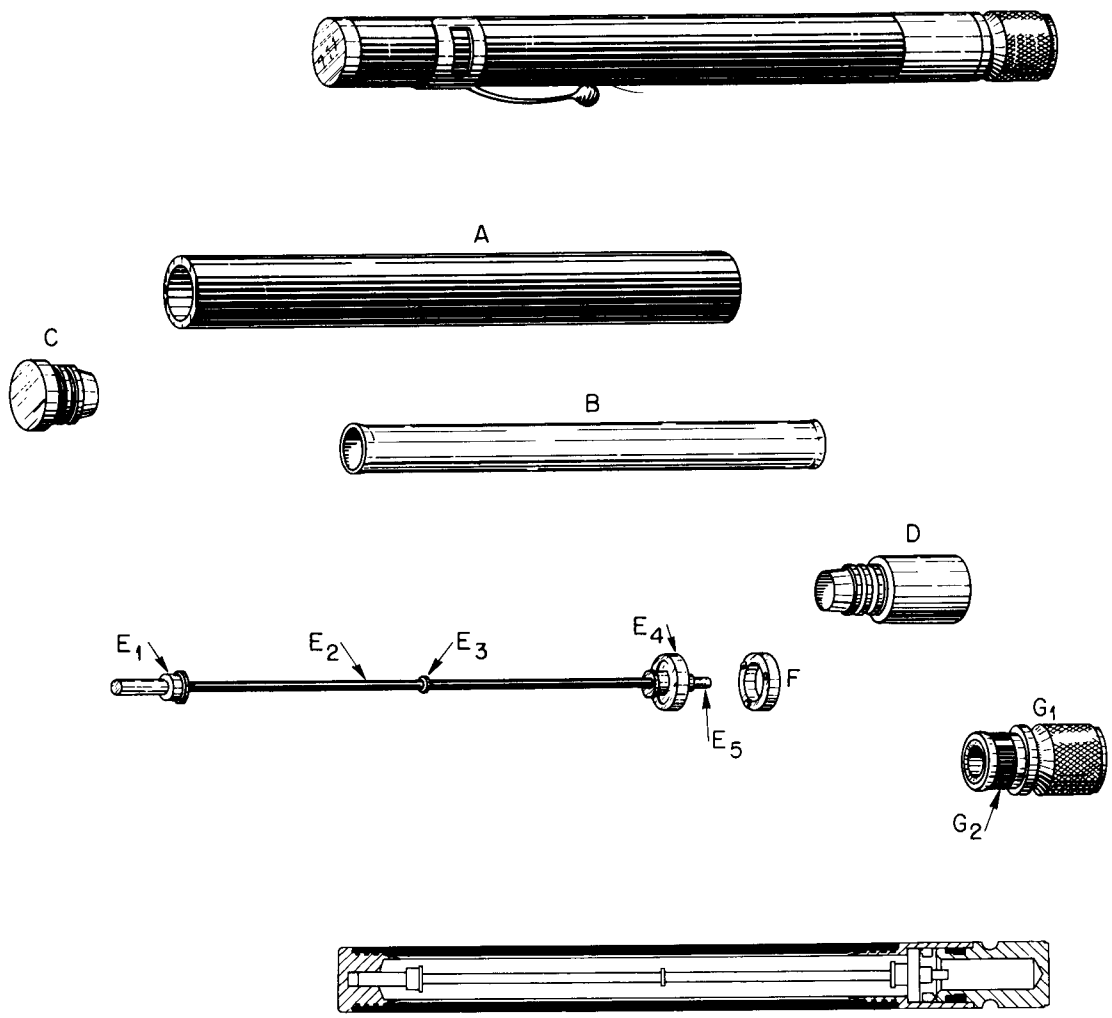

VICTOREEN POCKET METER, MODEL 362

A. LOW ATOMIC NUMBER WALL
B. GRAPHITE-COATED PAPER SHELL
C. ALUMINUM TERMINAL HEAD
D. ALUMINUM TERMINAL SLEEVE
E_1 POLYSTYRENE SUPPORT BUSHING
E_2 CENTRAL ELECTRODE, GRAPHITE COATED
E_3 POLYETHYLENE INSULATING WASHER
E_4 POLYSTYRENE FIXED BUSHING
E_5 ELECTRODE CONTACT
F. RETAINING RING
G_1 ALUMINUM BASE CAP
G_2 POLYETHYLENE FRICTION BUSHING

FIG. 12

UNCLASSIFIED
DWG. D-10499

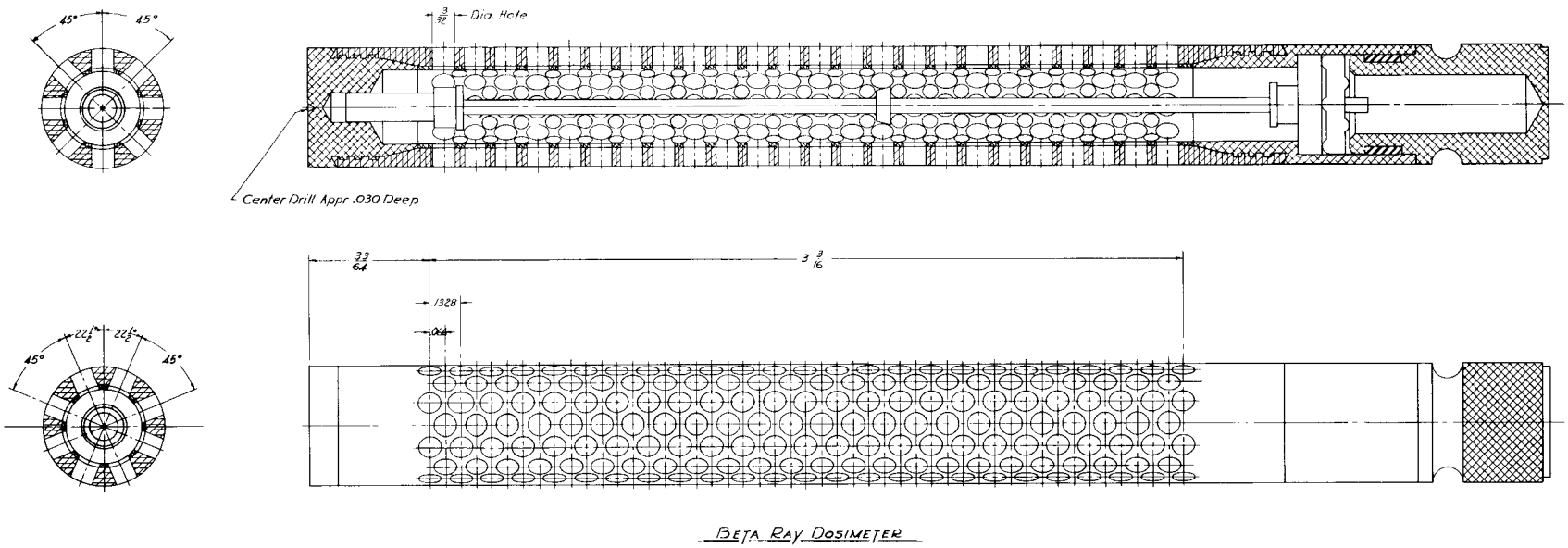

Fig. 13. Drilled Plastic Wall Pocket Chamber.

UNCLASSIFIED
HP-17-D-199

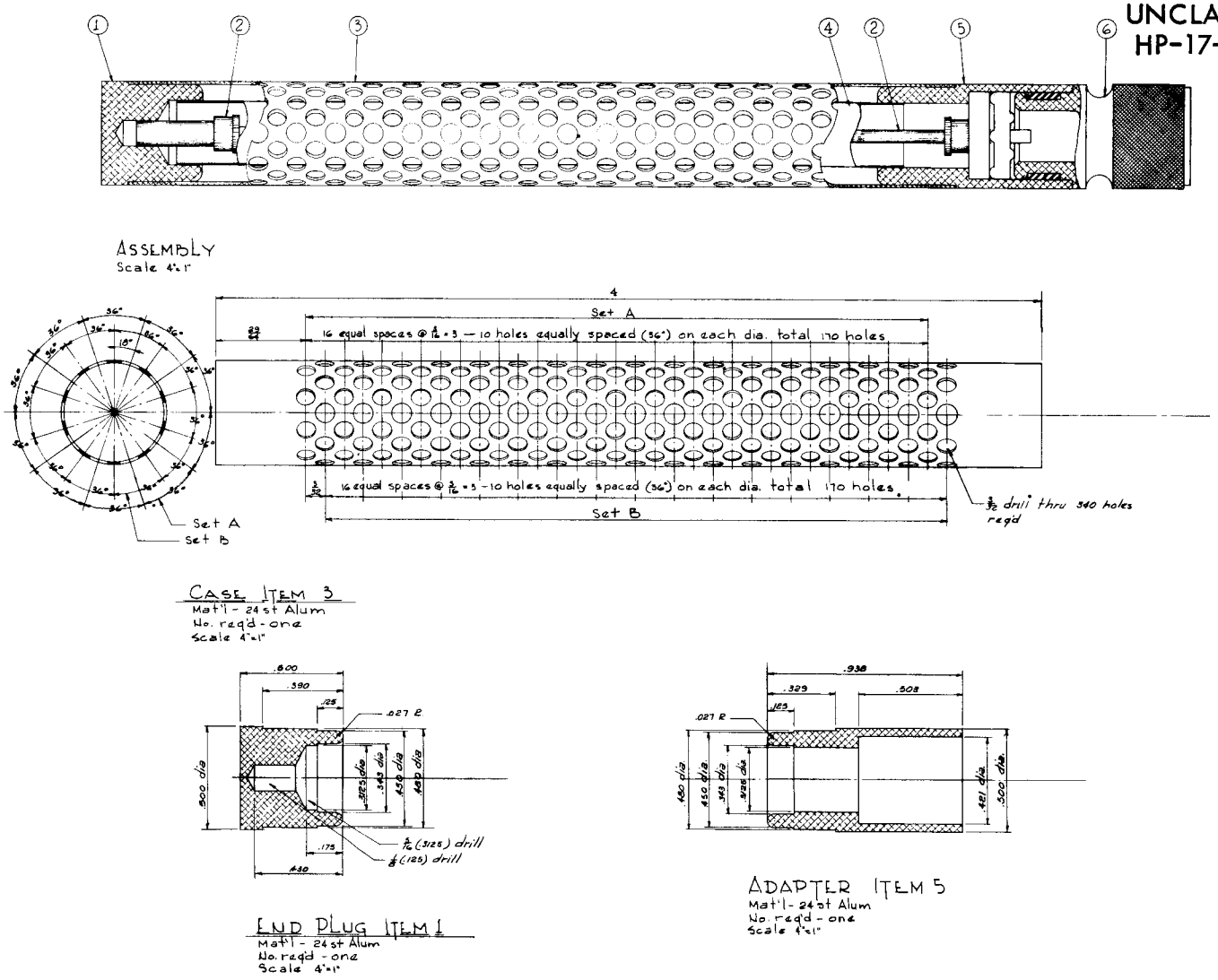

Fig. 14. Aluminum or Magnesium Wall Pocket Chamber.

holes would be uniform from pencil to pencil. The central volume wall might either be installed later, or molded into the plastic.

All pencils were read on a standard Victoreen Minometer, Serial SN287-1742, which was left operating continuously from a constant voltage transformer. This procedure served to minimize any fluctuations due to temperature changes, warm up, or line voltage changes. The milliroentgen scale on the Minometer was calibrated with an electrostatic voltmeter (see Fig. 15), and it was found that the zero reading was 135 volts rather than the usual 150 volts. After some thought the conclusion was reached that the actual voltage was of little importance so long as it was sufficient to produce voltage saturation of the chamber (collect all the ions), the argument being as follows: After a pencil has been charged and then irradiated, let the charge and voltage on the pencil be q and v, respectively, and let Q and V be the charge and voltage of the Minometer before insertion of the pencil. Then after the two have been joined again let q' and v' be the charge and voltage on the pencil and Q' and V' be the charge and voltage on the Minometer. We know that after they are joined,

$$v' = V' \quad . \tag{18}$$

At all times the charges are equal,

$$Q + q = Q' + q' \quad . \tag{19}$$

UNCLASSIFIED
ORNL-LR-DWG. 19081

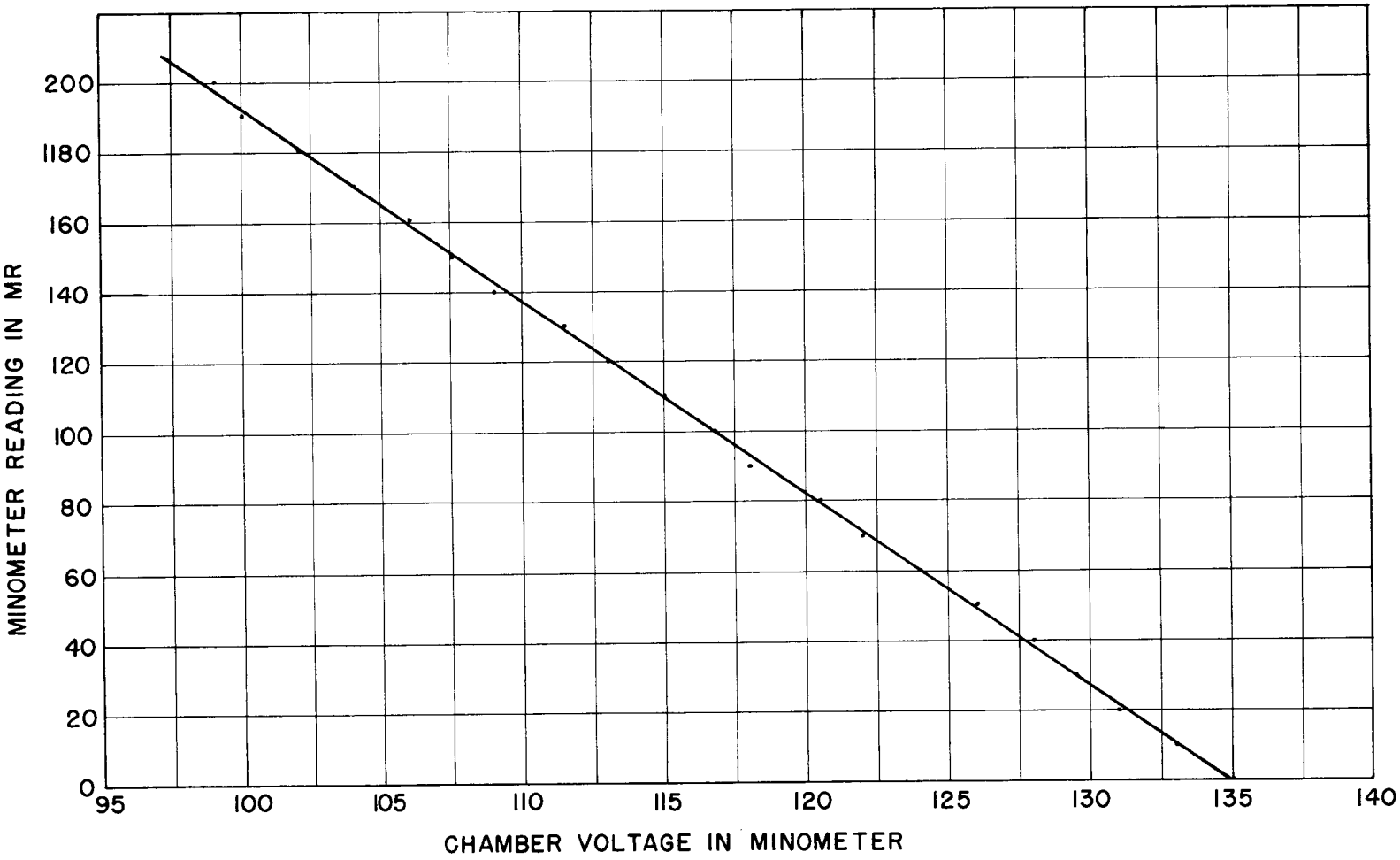

FIG. 15
VOLTAGE CALIBRATION AND SCALE LINEARITY IN MINOMETER 287—1742

The loss of voltage on the pencil due to irradiation then is

$$\Delta v = V - v = \Delta q/c \tag{20}$$

where c is the capacitance of the pencil. Then from Eq. (19) and $Q = CV$, we get

$$VC + vc = V'C + v'c \tag{21}$$

which from Eq. (18) equals

$$VC + vc = V'(C + c) \tag{22}$$

where C is the capacitance of the Minometer. The change read on the meter is

$$\Delta V = V - V'. \tag{23}$$

Then by adding and subtracting Vc to the left of Eq. (21) or Eq. (22) we get

$$V(C + c) + c(v - V) = V'(C + c) \tag{24}$$

which is simplified using Eq. (23) to give

$$\Delta V = -c(v - V)/(C + c) = \Delta vc/(C + c). \tag{25}$$

This shows that the voltage change read on the Minometer is directly proportional to the voltage loss in the pencil. Now a given amount of radiation will discharge Δq coulombs from the pencil,

$$\Delta q = c\Delta v \ . \tag{26}$$

Now, since we are at saturation[15] Δq is a function of the irradiation only, c is a constant so Δv is independent of V. Therefore, from Eq. (25) ΔV is independent of V; that is, it makes no difference what the initial voltage of the Minometer and chamber were.

---

[15] The pencils are sufficiently saturated at any voltage above about 50 volts to be within about 90% accuracy at dose rates of up to 8000 r/hr. See, Edwin D. Gupton, "Recombination Losses in Pocket Ionization Chambers," a thesis, Vanderbilt University, Nashville, Tennessee (1955).

3. Apparatus for Measuring Gamma- and X-Ray Response of Pencils

The irradiation of the pencils with low energy gamma rays was done by a standard 250 kilovolt Westinghouse Quadrocondex x-ray machine. The beam was heavily filtered, the filtration being approximately that suggested by Ehrlich and Fitch.[16] The table of filters and effective x-ray energies is given in Table I. The x-ray responses of the beta pencils were obtained under conditions where the gamma rays were in equilibrium with their secondary electrons by having the source at some distance from them. A thick plastic plate behind the pencils produced backscattered radiation, thus simulating actual wearing conditions.

The gamma response point at 700 kev was obtained by use of the standard radium gamma calibration rack at the Health Physics Calibration Building at Oak Ridge National Laboratory. For the radium exposures the source-dosimeter distance was fixed at 15 cm, so that the desired equilibrium was not quite reached.

The dosimeter used in obtaining the dose rates from the x-ray machine was a Standard Free Air Chamber of a type very similar in construction to the chamber at the National Bureau of Standards[17]

---

[16] M. Ehrlich and S. H. Fitch, "Photographic X- and Gamma-Ray Dosimetry," Nucleonics 9, No. 3, 5 (1951).

[17] (a) Research Paper No. 56 (1928), Dept. of Commerce, Bureau of Standards, Washington, D. C.; (b) Lauriston S. Taylor and George Singer, "An Improved Form of Standard Ion Chamber," read before the Radiological Society of North America, Toronto, December, 1929; (c) Research Paper No. 865, p. 16, Vol. 16, J. Res. National Bureau of Standards, Washington, D. C. (Feb. 1936).

Table I

Standard Filter Combinations and Kilovoltages

Applied Kilovolts	Filter Components				Effective Kilovolts
	Lead mm	Tin mm	Copper mm	Aluminum mm	
30	-	-	-	0.49	21.5
50	-	-	0.26	0.49	34.5
76	-	-	0.938	0.80	46.5
100	0.48	-	-	1.03	71
150	-	1.19	3.12	1.03	116
200	0.63	2.55	1.07	1.03	165
250	2.081	1.18	1.07	1.03	191

(see Fig. 16). An accurately machined lead diaphragm, S, fits into the lead block and defines the cross sectional area of the cone of radiation from the source, C. The length of the volume of air, V, is fixed by the length of the collecting plate, K. The current measured per unit volume then gives the roentgens per second to the center of the volume. Using the inverse square law, it is easily seen that this reading in roentgens is the same as that which would be obtained in a cylinder of diameter equal to that of the shield opening S, centered at the point S. To assure a uniform parallel electric field between the high voltage plate, H, and the collecting plate, K, use is made of guard plates, L, and a potential dividing system of wires, w, spaced around the collecting volume and connected to a resistance voltage divider. The source cone, C, was confined and collimated by a thick lead shielding (not shown) to minimize scattered radiation in the room, and the collecting volume was similarly enclosed in a heavy lead cell to eliminate scattered radiation. The beam was conducted out the end of the chamber for a distance of about one yard and trapped in a deep lead well to minimize backscattering. A sheet of very thin conducting plastic, P, was located at the exit of the shielding portion of the chamber to prevent air currents or drafts from carrying ions back into the sensitive volume. The arrows and wavy lines (see Fig. 16) show typical paths of the secondary electrons.[18] Thus

---

[18] For energy and intensity distributions of both Compton and photoelectrons, see Figs. 6-10 and 6-11 in HEALTH CONTROL AND NUCLEAR RESEARCH by K. Z. Morgan (to be published).

UNCLASSIFIED
ORNL-LR-DWG 15723

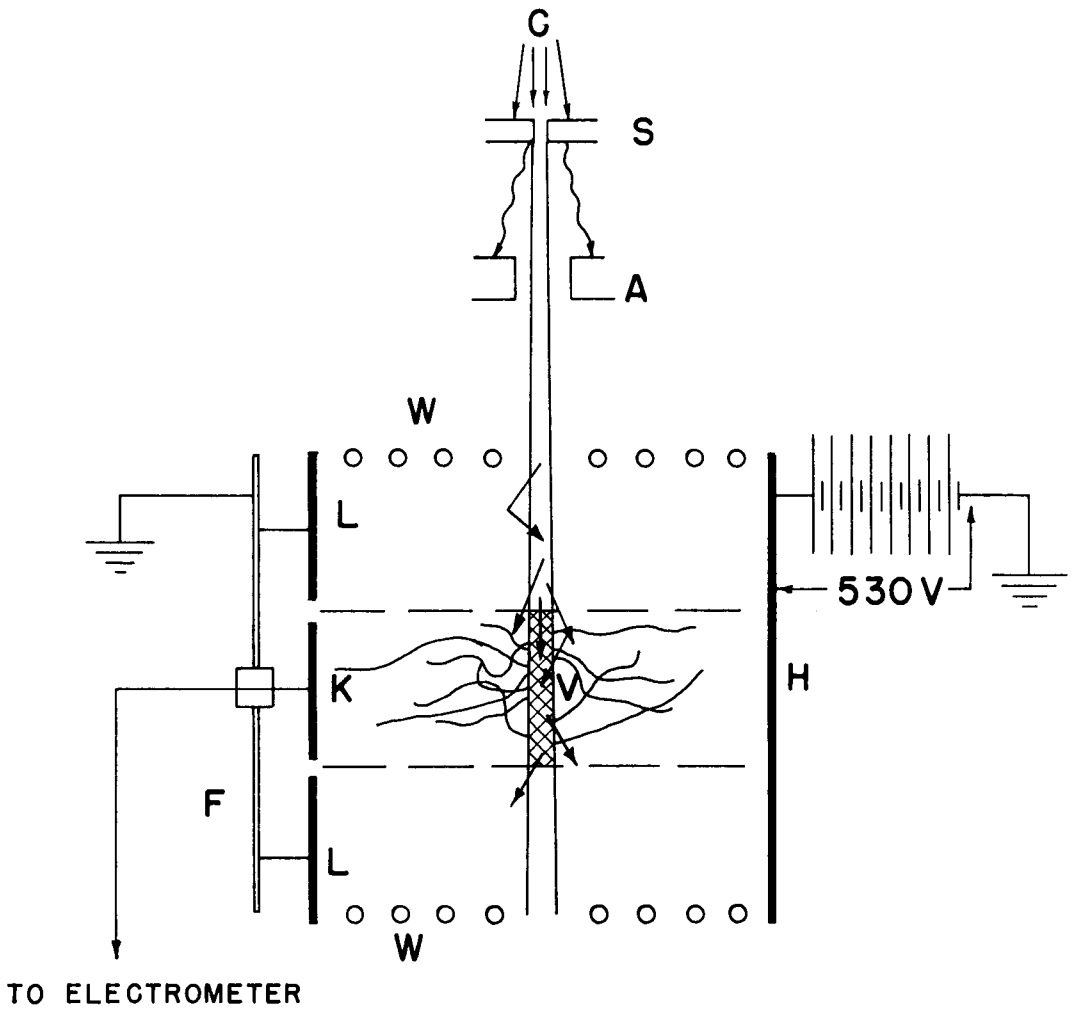

FIGURE -16

STANDARD FREE AIR CHAMBER DIAGRAM

there is as much energy gained in the dotted collecting volume between K and H by electrons with tracks entering that volume from outside as is lost by electrons that start in volume V but leave. This condition is approximately met if the distances from K and H to V are greater than the maximum range of the secondary electrons and the source and shields are at a distance from volume V equal to the maximum range of the secondaries. Saturation was checked with potentials up to 530 volts across the plates of the standard free air chamber. Readings were made both with and without a lead stop covering the diaphragm, S, in order to check for scattered and stray radiations.

The arrangement of x-ray head, standard air chamber, and pencils is shown in Fig. 17.

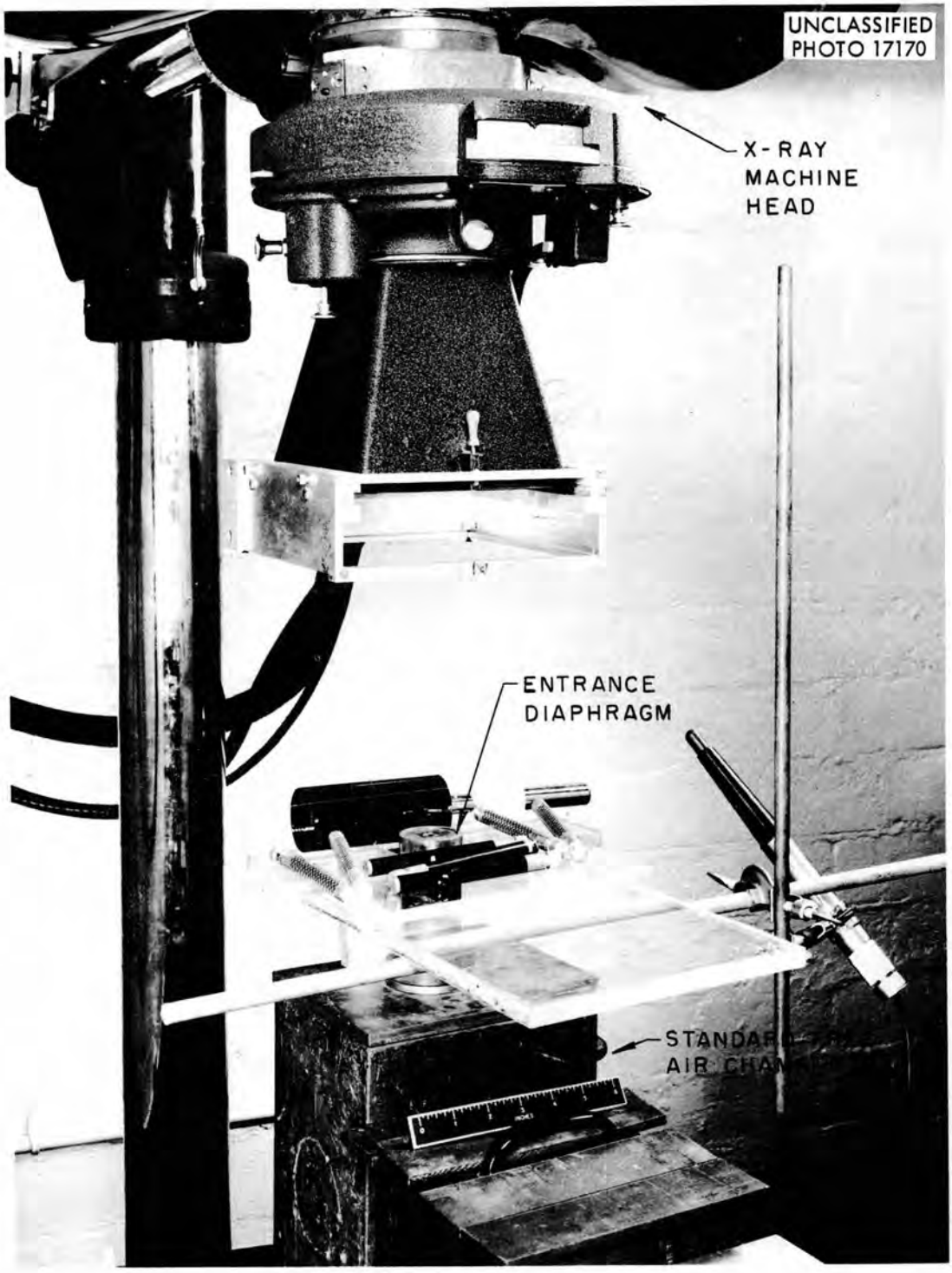

FIG. 17- X-RAY EXPOSURE ARRANGEMENT

4. Isotopes Used

A series of isotopes were chosen to get as wide a range of beta energies as possible for calibration of the pencils. Table II gives the isotopes used, their maximum energies, average energies, and the average energy of their spectra in water solution.

The isotopes used in this experiment were chosen on the following basis. The first consideration was given to obtaining pure beta emitters whose maximum energies covered the spectrum as uniformly as possible. Careful thought was also given to trace contaminants (alpha or gamma emitters), ease of handling, and solubility of the required salt in a water medium. The half lives were chosen long enough wherever possible to permit an adequate range of working time and yet short enough so that a spill would not cause a permanent contamination. The decay schemes were noted so that there would be no interference from the daughters. An attempt was made to keep the amount of solid matter in the solution down to a very low level to increase the accuracy of the assay since the half thickness for the very lowest energy betas is in the range of a few micrograms per square centimeter, and an appreciable amount of solids renders the counting very difficult and inaccurate, if not impossible.

Table II

Average Energies of Isotopes

Isotope	Maximum Energy Beta Mev	Average Energy Beta Kev $\overline{T}_N$	Average Energy* of Electron Spectrum in Water Solution $\overline{T}_y$	% Dose Due to Plated Activity	Average of Electrons in Cavity Including Plated Activity
Y^{90}	2.19	900 ± 5%	694 kev	0	694 kev
P^{32}	1.701	690 ± 2%	506 kev	13.1	530 kev
Ag^{111}	1.04	370 ± 10%	317 kev	0	317 kev
Tl^{204}	0.77	243 ± 3%	237 kev	7.5	237 kev
W^{185}	0.43	134 ± 10%	130 kev	15	131 kev
Ca^{45}	0.25	80 ± 20%	79 kev	0**	79 kev
S^{35}	0.167	55 ± 5%	52 kev	80	54 kev

* Calculated from Spencer-Fano-Attix theory (Ref. 5).

** Calcium plated on the glass storage bottle but apparently not on the Mylar film used.

5. Plating Problems

One of the many problems encountered using radioactive solutions with trace amounts of radioisotopes is that the activity seems to concentrate or plate on the container surface. This concentration of activity is due to three primary causes: first, electrochemical action; second, a radiocolloidal effect; and third, an adsorption or ion exchange type reaction in the plastic of the chamber wall.[19]

The electrochemical action is the familiar condition where an active metal is dissolved by a solution and a more electronegative (more noble) metal replaces it, plating from the solution. This effect can be reduced by introducing some of the electrode metal ions into the solution. The radiocolloidal effect is merely a micro precipitation and can be reduced by choosing radioactive materials in forms that have as high a solubility constant as possible, and by keeping the concentration low. The adsorption effect is present at all times with any solution but is of such a minute amount as to be undetectable except where the ions adsorbed are radioactive. This last situation is bad especially where there are only a relatively few ions in solution, as with a carrier-free isotope. In this case, the number of ions adsorbed amounts to a significant percentage of the total. The effect may be lessened by presoaking the surface in a solution of the nonradioactive ion, and by adding carrier to the solution. This is somewhat counter to

---

[19] G. K. Schweitzer and W. M. Jackson, J. Chem. Ed. 29, 513 (1952).

the requirement of low concentrations to keep the radiocolloidal effect minimized, but the third effect is orders of magnitude greater than the second in most cases, so the use of carrier is advised.

In this experiment several methods were used to try to overcome the plating problem. The first and most obvious involved controlling the pH of the solution to insure redissolution and to prevent any formation of a precipitate or colloidal suspension. An early, unsuccessful method of correcting for plating involved a radio-assay before the use of the isotope and again after the measurements had been made. After correction for decay the difference between the assays should have indicated any marked loss of activity of the medium, but in practice it only served to underscore the difficulty of obtaining an accurate assay on the low energy beta emitters. The method was rejected since the loss in activity was less than the probable error of the count.

To determine the amount of plating the radiation from the solution was measured by converting the chamber into an ionization chamber as mentioned above. After taking the Mylar ionization chamber readings the cell was drained, and the outer walls rinsed to remove any remaining radioactive solution. Care was taken not to rinse the Mylar. Then the cell was refilled with a buffer solution composed of the nonradioactive element in the same chemical form, concentration, and pH as in the radioactive solution. The readings taken at this time gave a reasonable idea of what percentage of the radiation in the cell was due to the degenerate spectrum of the solution and what percentage was due to the thin source

spectrum of radiation from the plated material. If the spectrum in an infinite radioactive solution is desired, free of the thin source spectrum, it is desirable to presoak the cell for several days in a buffer solution containing a concentration of nonradioactive element in excess of that to be used in the radioactive solution, and acidified to two or three normal with the acid of the salt used. This would tend to infuse the Mylar with the element and to minimize later plating of the radioactive isotope. The wall of the central volume should be made conducting with gold on both sides rather than with aluminum, and the final solution should have a large percentage of carrier added to the isotope immediately after removal of the sample to be radio-assayed. With proper choice of pH these steps should reduce the plating to a negligible amount. The next to the last column in Table II gives the percent of the dose rate in the cell which is due to the plating in each case. These figures are for solutions of admittedly differing concentrations and pH values.

In a permanent setup where the several solutions would be used, each in its individual cell, plating might be an advantage rather than a disadvantage since its effect would be to superimpose a percentage of the thin source spectrum on the normal flux spectrum in the solution which we calculated from the Spencer-Fano-Attix theory. This would effectively flatten the flux curve of the radiation passing through the chamber.

The radio-assays* of the isotopes were performed by a method of

---

* We are indebted to H. A. Parker and W. S. Lyons for these radio-assays.

"absolute beta counting." In this technique the counting is done with a proportional counter, with the isotope mounted on a low backscatter polyethylene mount. The counting data is taken as a function of the thickness of aluminum absorber placed before the tube. These data are then extrapolated back through the air and window thickness to zero absorber and multiplied by the appropriate "geometry" factor to get the disintegration rate. For calcium and sulfur with their extremely low energy betas, the isotopes were counted directly on the 4π counter to minimize the unavoidably large error at these energies. For the estimated accuracy of the assays, see Table III.

Ideally, the experiment would be performed with one type of pencil at a time and with perhaps nine or more calibration cells, so that the complete response curve of any type of proposed beta dosimeter could be obtained in a relatively short time. Practical considerations, however, limited us to two cells. The first step after filling the cell and noting the time of immersion of the central chamber was to obtain a series of readings using the chamber as an ionization chamber. These readings were then plotted against time. If plating occurred the data could be extrapolated back to zero time to give an accurate basis for comparison with the theoretical value of the dose rate in the cell as it was calculated from the assay. The dose rates for the various pencils were then obtained in sequence by inserting the pencil into the cavity in the center of the radioactive medium for an accurately measured length of time. If necessary, correction was then made for the decay rate of the

Table III

Assay Information and Error

Isotope	Estimated Limit of Error %	Precision (95%) Confidence Level
Y^{90}	± 10	± 3
P^{32}	± 3	± 2
Ag^{111}	± 20	± 3
Tl^{204}	± 20	± 3
W^{185}	± 20	± 3
Ca^{45}	± 20	± 5
S^{35}	± 20	± 5

isotope, and the data for all pencils of the same type averaged together. The exposure times used were chosen so as to obtain readings approximately 3/4 of full scale. The results were then corrected for leakage drift and cosmic ray or background radiation where necessary. The cell was then used again as an ionization chamber to obtain a final point on the curve to check for plating. It was then emptied and rinsed out, great care being exercised not to rinse the central chamber, refilled with a buffer solution of the same concentration of nonradioactive isotope and another reading taken. This gave the exact percentage of the dose rate which was due to isotopes plated on the chamber. The chamber was then emptied, decontaminated, the surface of the stainless cell passivated with a solution of HNO_3, and a new Mylar wall for the central chamber installed and tested. Each of the isotopes was used in this fashion.

The next step was to check the response of the pencils for gamma radiation to determine how closely their response matched the response of the standard pocket chamber. The procedure was to put a tissue equivalent phantom around the entrance diaphragm, S, of the standard free air chamber and use it as a primary standard (see Fig. 17) while irradiating the pencils with x-rays. After installing the proper filtration for each energy, the x-ray beam was directed at the standard free air chamber until the observed reading had time to stabilize. The scattered and background radiation was then determined with the opening of the chamber plugged and the extent of the area of the x-ray field on

the phantom checked with a fluorescent screen and marked. Next the charged pencils were arranged on the phantom in such a manner as to minimize scattered radiation from one type of pencil to another. Sufficient irradiation was then given to discharge the pencils to three quarters of a full scale reading, and simultaneously the dose rate was rechecked with the standard free air chamber. This procedure was repeated for the remainder of the pencils, irradiating at the same time the secondary standard, with each set of pencils. The pencils were then read on the Minometer to the usual $\pm$ 10% accuracy and carefully reset to zero. The secondary standard used in this experiment was a Victoreen Condensor R-Meter, Model 70, Serial No. 2913, with a 0.25 r chamber. This chamber was used as a primary standard for the gamma readings above 200 kev where the standard free air chamber is too small to collect all the secondary electrons. During exposure to the radium source the pencils were again backed with a phantom made of 3/4 inch Lucite sheets and were exposed long enough to give approximately a 3/4 full scale reading. These x- and gamma-ray exposures were all repeated, changing the pencil center wires from the original type which was fully coated with graphite to the newer half-coated center wires. All of the resulting response curves for the beta pencils were surprisingly close to the curve of the standard Victoreen gamma sensitive pocket pencil.

IV. EXPERIMENTAL RESULTS

1. Beta-Ray Calibration of Pocket Chambers

The results of the calibration of the various types of pocket chambers are summarized in Figs. 18, 19, and 20. At the top of each graph are given the isotopes used and the average energies, $\overline{T}_y$, of the electron fluxes in each case.

In Fig. 18 the observed dose rates are compared with those calculated on an absolute basis for each isotope from its measured concentration. Several points of basic physical interest are evident. The curve for the ionization in the Mylar wall chamber, that is, in the cavity itself, shows that for high energy electrons the dose rate is given correctly by the Bragg-Gray principle. The deviations found by Gray and Spencer-Attix are too small to be observed within the accuracy of these measurements, and in any case would not arise here where the cavity gas and its walls all have low atomic numbers.

In addition this curve shows that even a 1 mg/cm^2 absorber (the Mylar) produces a reduction in dose rate to 94% of that calculated at 700 kev average electron energy and to about 63% at 79 kev. The additional 7 mg/cm^2 in the wall of the paper chamber cuts this dose rate down to 14.7% at 79 kev and 9.5% at 52 kev average electron energy. The loss is surprisingly large since the range of 52 kev electrons is about 6 to 8 mg/cm^2, and one would expect that electrons in the medium having an energy higher than this average would have longer ranges.

Our observation that, contrary to the arguments just given, most

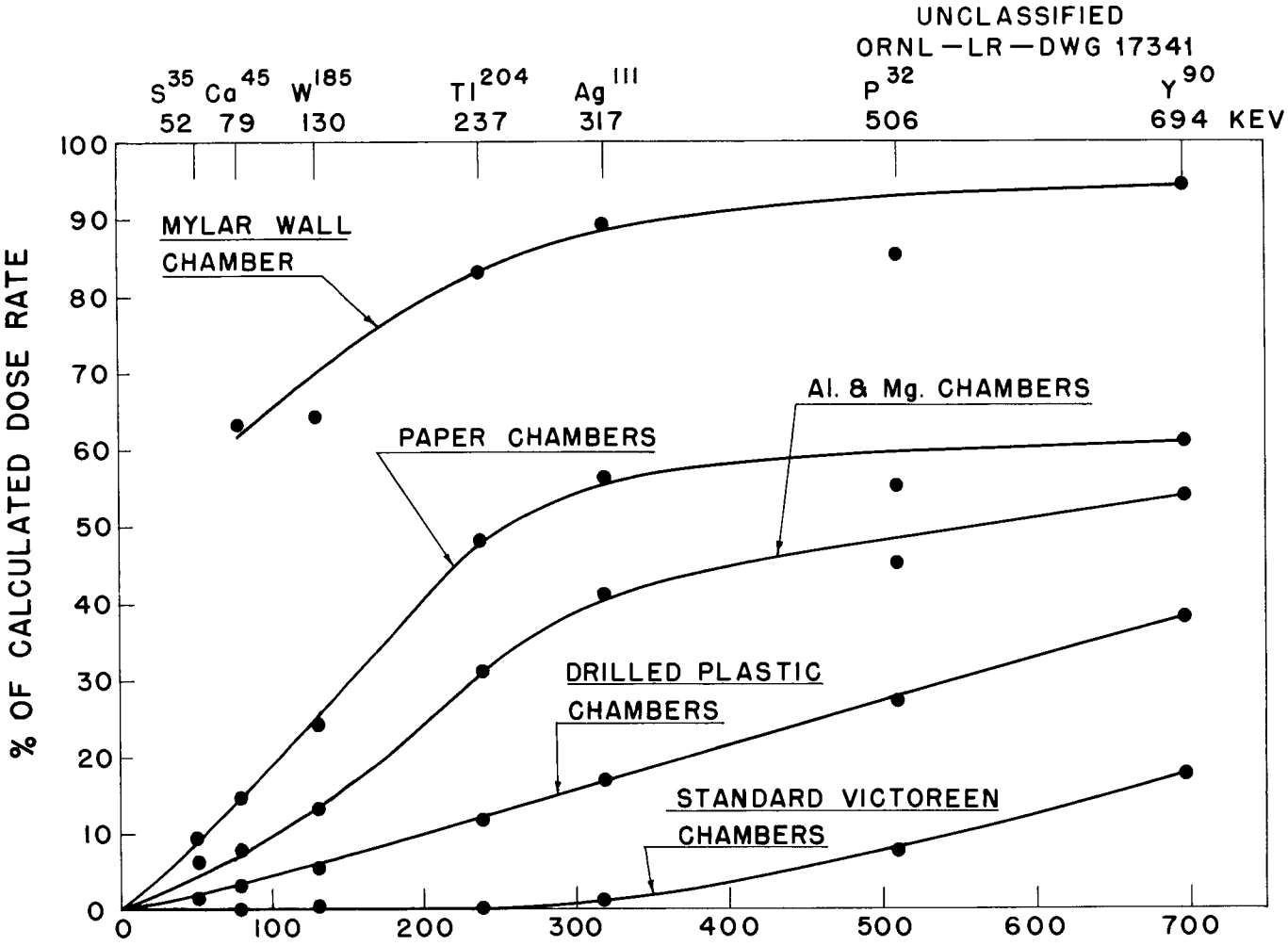

FIG. 18 - RESPONSE OF CHAMBERS COMPARED TO THAT CALCULATED

of the dose is deposited at very small depths of penetration shows the great importance of the build up of low energy secondaries and the large proportion of the total dose they deposit. This secondary flux is indicated on the curves, Figs. 1 - 7, by the sharp upturn and steep rise in the flux spectra y(T) below 10 kev. The high dose rate in the first 8 mg/cm^2 of absorber then represents the large fraction of the total dose carried by this sea of low energy electrons.

This flux spectrum has been measured recently and agrees well with that calculated down to at least 50 kev. The work has been reported[20] and will be described elsewhere.

The curves for the drilled plastic chambers and the aluminum and magnesium walled chambers, which are also drilled, show that, as was expected, the low energy electrons can only enter the ionization chamber through the holes, while the high energy electrons also penetrate the solid parts of the outer shells and still contribute to the dose in the chamber. Since the plastic material is weaker mechanically, its wall must be much thicker (.088") than the metal walls used (.010"). As a result, electrons can reach the ionization chamber of the drilled plastic chamber only if they are initially directed toward the pencil axis and within a small cone about a normal to it. Electrons striking

---

[20] Birkhoff, Cheka, Hubbell, Johnson, and Ritchie, "Measurement of Electron Flux in a Radioactive Medium," Bull. Am. Phys. Soc., Ser. II, Vol. 1, No. 4, p. 184 (1956).

the chamber at angles outside this cone will penetrate varying amounts of plastic and have their energies lowered by varying and unknown degrees before being recorded. This penumbra effect gives the response a strong angular dependence, which is undesirable.

Electrons can reach the sensitive volume of the Al or Mg walled chambers from a much wider cone; hence the higher sensitivity of these pencils at low energies, even though the total superficial area of the holes was practically the same for the metal and plastic walled chambers.

There was no significant difference in the response of pencils with magnesium walls, pure (2S) aluminum walls, or alloy (24ST) aluminum walls so the data for all three have been averaged.

The responses of the various types of pocket dosimeters are compared with the measured ionization in the cavity in Fig. 19. The dose rate in the Mylar walled cavity as shown in Fig. 18 does not seem to extrapolate to zero at zero electron energy, probably because the radioactive solution infuses into the Mylar to some extent so that some beta rays are emitted practically at the concave wall of the cavity. This infusion is, however, not sufficient to raise the Mylar walled chamber dose rate to that calculated. Since the dose in the cavity thus remains finite for very low beta energies, while those in the pencils certainly approached zero, we have drawn the curves for the pencils through the origin.

This Mylar wall represents the thinnest practical wall a dosimeter could have, and even this wall does not give a dosimeter with 100% response. The Mylar walled chamber also permitted a measurement of the effect of

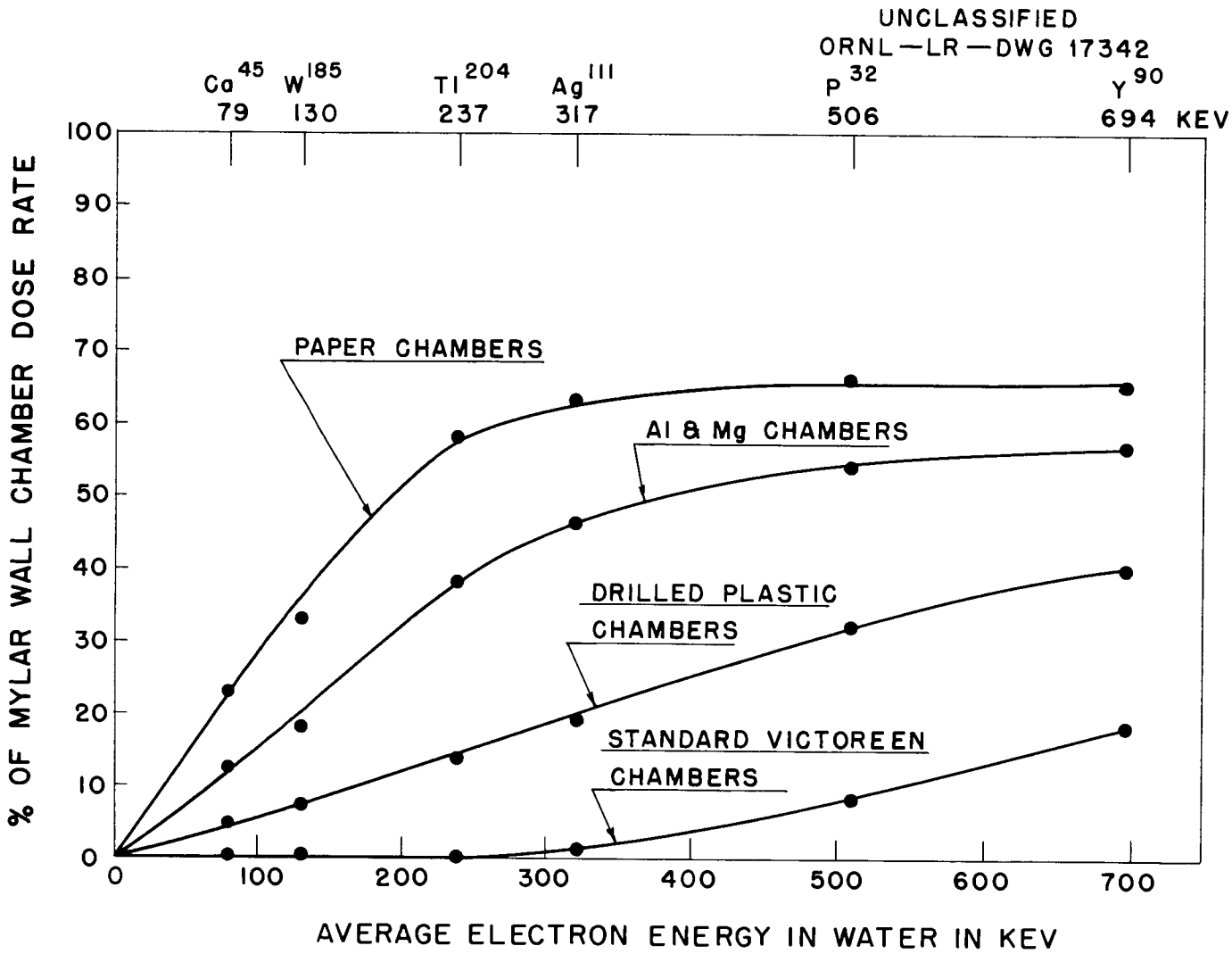

FIG. 19-RESPONSE OF CHAMBERS COMPARED TO MEASURED IONIZATION IN CAVITY

plating of the radioisotope on the walls of the cavity, as discussed above.

Fig. 18 gives the answer to the question of how much of the beta ray dose present will be recorded by the various pocket chambers. From the health physicist's viewpoint, a more important question is how much of the dose reaching the basal layer of the human epidermis is recorded by the dosimeter. To answer this question the data on the pencils shown in Fig. 18 are replotted in Fig. 20. The assumption is made that any dose recorded in the paper walled chamber will reach the basal layer of the epidermis. Hence in Fig. 20 the other chambers are compared to the paper walled chamber.

The Victoreen pocket chamber gives a negligible response to beta rays from isotopes whose maximum energy is below 1 Mev, as is evident from the points on Figs. 18 - 20 for Ag^{111} whose T_o = 1.06 Mev. The walls of the Victoreen chamber are too thick for beta dosimetry, and it was never designed or intended to measure beta rays. The drilled plastic chamber offers a definite improvement. Its response ranges from 20% of the dose seen by the skin up to 60%. This pencil could serve as a reasonable dosimeter for beta rays if its readings were multiplied by three. The average curve for the magnesium and aluminum walled pencils shows a response that ranges from about 55% of the dose to the basal layer of the epidermis at 55 kev to 90% of the dose at 650 kev. This pencil could be used for pure gamma radiation as is or read for pure beta dose with a reasonable safety factor if its readings were multiplied by

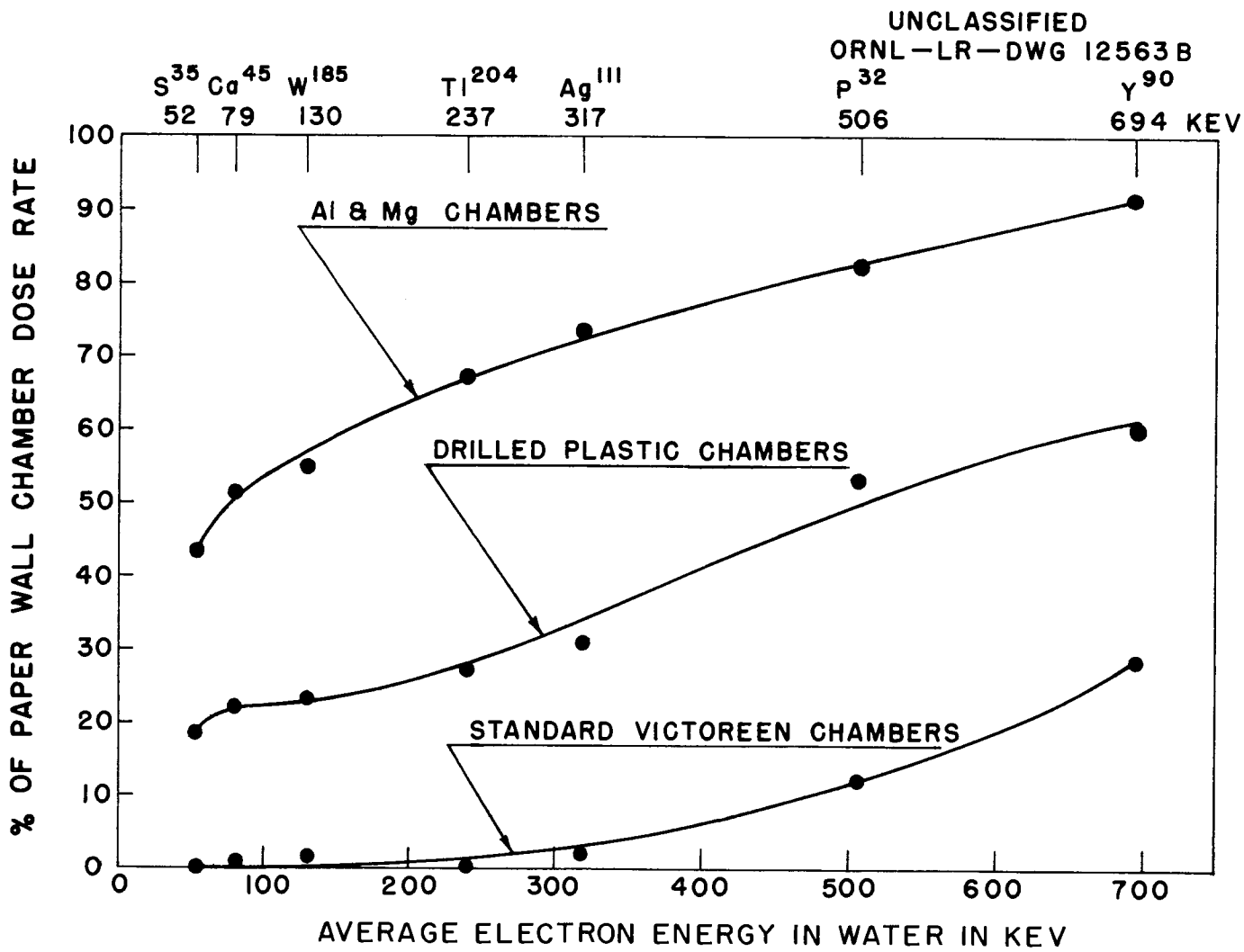

FIG. 20-RESPONSE OF CHAMBERS
COMPARED TO PAPER WALL CHAMBER

two. The advantages of the perforated metal walled pencil over the drilled plastic pencil are the former's lack of angular dependence, its higher sensitivity, and its smaller attenuation of beta rays striking the metal walls at angles to the axis.

If the readings of the aluminum wall chamber are taken simultaneously with those of a standard Victoreen pocket chamber, the beta dose is easily estimated by subtracting the Victoreen gamma reading from the aluminum chamber reading and multiplying the remaining number by a factor of two. This method will give a safety factor to the determination that could be reduced at the discretion of the health physicist using the pencils. However, since the maximum permissible exposure for beta radiation (that is, MPE for dose to skin alone) is twice that for gamma radiation, the aluminum chamber reading may be expressed as a per cent of the permissible exposure to mixed beta and gamma rays.

2. Gamma and X-Ray Response of Pocket Chambers

The chambers were irradiated with gamma and x-rays as described previously, and the results are shown in Figs. 21 - 24. Our curves show a narrower peak around 45 kev than Day[4] obtained. His results are shown in Fig. 21 as a dotted curve.

Except at the peak the chambers agree with each other within the accuracy of the experiment. Our chambers seem to show a lower response peak around 45 kev than the standard one, for reasons that are not clear.

There was no significant difference in the response to gamma and x-rays of the pencils made with magnesium, 2S aluminum, or 24ST aluminum alloy, but stainless steel gave large variations and was rejected.

For the radium source the pure paper walled chamber dropped slightly in efficiency, although it did not drop as much as had been expected. Contrary to expectations, the chamber with the aluminum outer shell had a response similar to the Victoreen chamber shell. Apparently, the photoelectrons which give a peak at 45 kev are absorbed by the chamber wall so that there is no appreciable effect on the measured dose.

The difference between the half coated center electrode and the fully coated one is seen by comparing Figs. 21 and 22. It may be seen directly for the special cases of the Victoreen and the average of the Al-Mg pencils in Figs. 23 and 24. The indication is that the older, fully graphite coated, center wires are superior if one wishes to reduce a spurious high reading for exposures in gamma and x-ray fields with energies in the region of 30 to 110 kev. The half coated electrodes also lacked the insulating lead in the center and are therefore more likely to discharge when dropped.

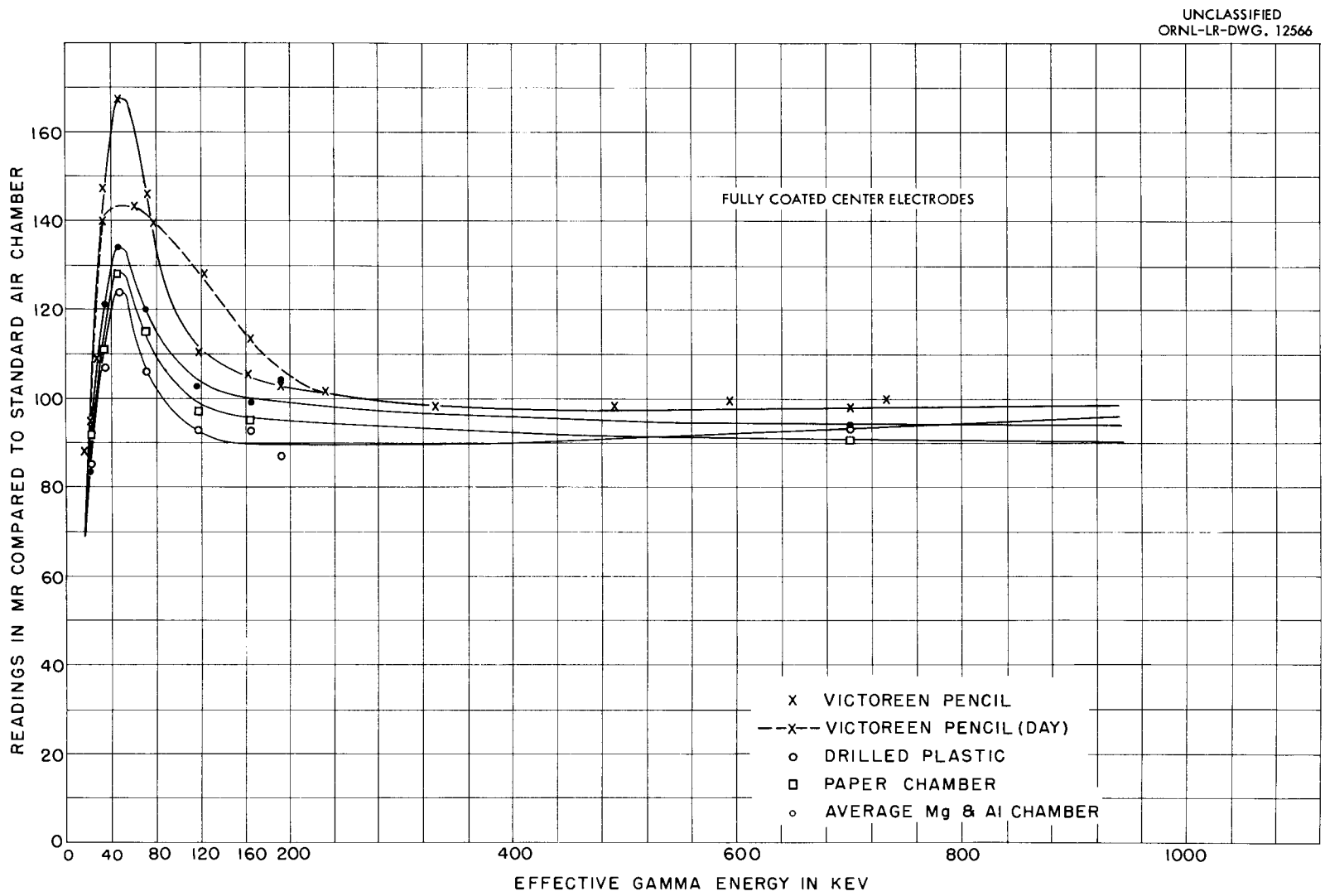

FIG. 21- GAMMA RAY RESPONSE OF CHAMBERS I

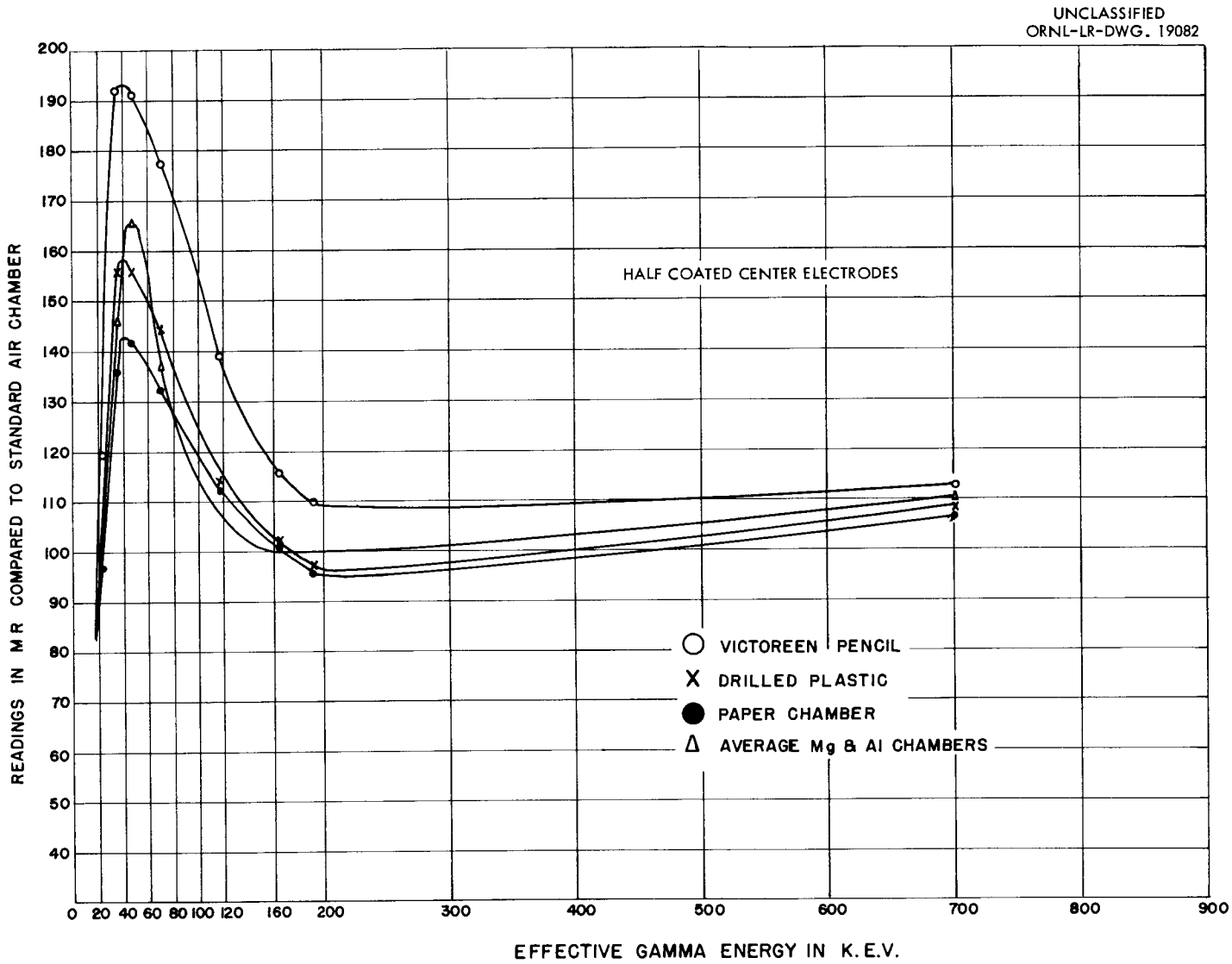

FIG. 22- GAMMA RAY RESPONSE OF CHAMBERS II

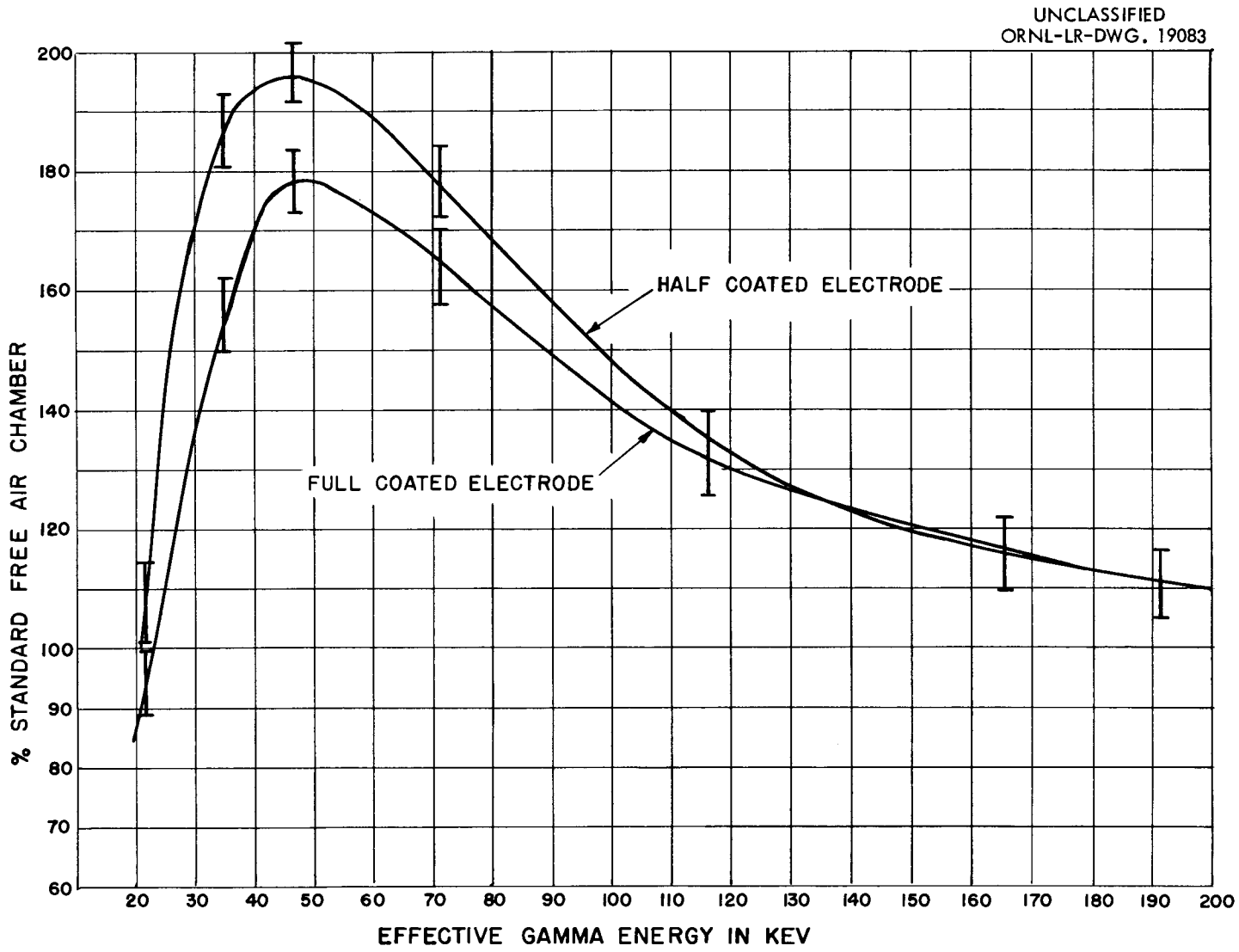

FIG. 23- ELECTRODE COATING EFFECT ON GAMMA RESPONSE OF VICTOREEN CHAMBER

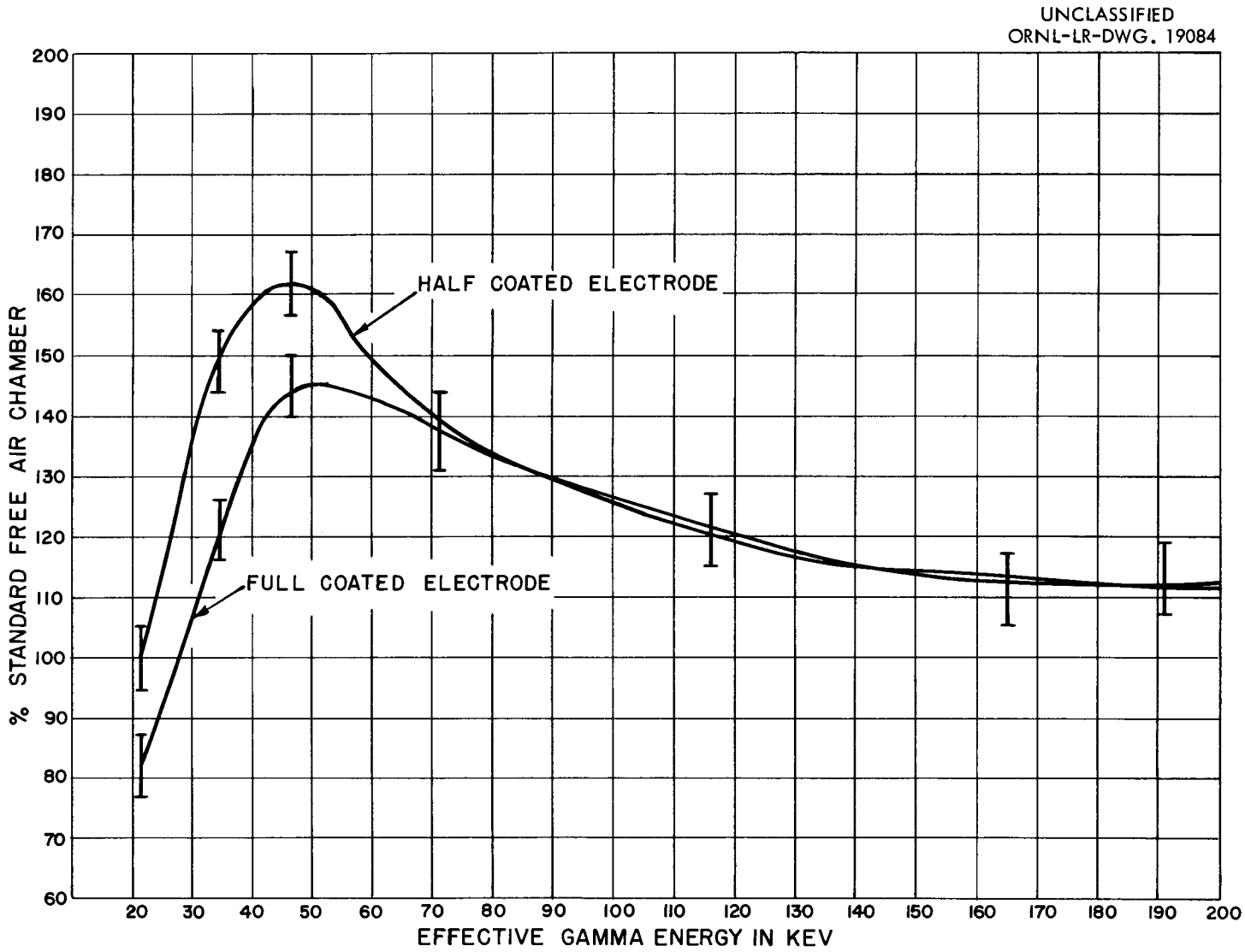

FIG. 24 - ELECTRODE COATING EFFECT ON GAMMA RESPONSE OF DRILLED AL CHAMBER

3. Errors and Estimated Accuracy

The thin source spectra calculated in this work and shown in Figs. 1 - 7 are probably correct within ± 10% at the upper end except for Y^{90}. The bump in the spectrum of Y^{90} around 1.2 Mev seems to have been exaggerated by the methods used. The thin source spectra at their lower ends are much more uncertain, especially that for W^{185}. However, the exact shapes of these curves have very little effect on the average energies obtained, $\overline{T}_N$, or in the integral primary spectrum which is used to calculate the flux.

The flux spectra are affected somewhat more strongly by the approximations used in the Spencer-Attix calculation as discussed under THEORY and in the APPENDIX. The results are probably accurate to ± 5% at the higher energies, but may be off by 20% or perhaps more at low energies as evidenced by recent experiments.[20] Again, however, the average electron energy in the flux, $\overline{T}_y$, will be very little affected by such errors, since it depends only slightly on the shape of the spectrum in the low energy region.

The experiment was planned to develop a practical dosimeter and therefore was not expected to yield results closer than ± 10%. By correcting the "zero kick" and averaging the results of at least four pencils, the curves are probably accurate to ± 5% in the cases of Figs. 19 and 20. The estimated limits of error for assaying beta solutions is generally ± 20% (see Table III, p. 50) so that the ordinates in Fig. 18 are only valid to that limit of absolute error. The internal self

consistency in these curves is better than this. The gamma and x-ray response curves are likewise probably good to $\pm$ 10% or better.

V. DISCUSSION

The maximum permissible weekly dose as set forth in the National Bureau of Standards Handbook No. 59[21] is 0.300 rem (roentgen equivalent man) for penetrating radiation (gamma) and 0.600 rem for radiation that does not reach the blood forming organs (beta and soft x-ray). Therefore, our pocket chamber was designed to measure approximately 50% of the beta dose. This means that the pencil gives a response that conforms to the standards set up for the protection of workers in the field of radiation, that is, the pencil is calibrated to read penetrating radiation directly in rem (under normal field conditions) and to read about half value for the skin dose (betas) for which the maximum permissible exposure is twice as great as it is for radiation which affects the blood forming organs. This means that the observed pencil reading might well be considered as the effective total beta and gamma dose, with a maximum permissible exposure of 0.300 rem.

The pencil has several definite advantages when compared to other usual means of personnel dosimetry. The most widely used instrument for personnel dosimetry is the film badge. The badge as used at Oak Ridge[22] is made of plastic with a total of 81 mg/cm^2 of low atomic number material

---

[21] Handbook 59, "Permissible Dose from External Sources of Ionizing Radiation," p. 76, National Bureau of Standards, Department of Commerce, Washington, D. C. (1954).

[22] Roy L. Clark, Health Physics Division, Oak Ridge National Laboratory, February 5, 1953 (unpublished data).

in front of the first sensitive layer of the film. This thickness is equal to the maximum range of a 320 kev electron, or approximately to the range of the average energy beta from Bi^{210}, a fairly "hard" beta (E_m = 1.17 Mev). At the back of the badge the shielding is even greater, for the absorber shielding in front of the first layer of sensitive film is 186 mg/cm^2 thick, or approximately 27 times as thick as the wall of our pocket ion chamber. This is equivalent to the maximum range of a beta particle of 560 kev energy. Thus the pencil is far more sensitive to the low energy betas and has the additional advantage of giving a good measurement of dose received from soft x-rays, or the gamma rays from americium or other low energy gamma emitters. The film badge requires large corrections in this range, since for about 200 kev above the "K" absorption edge of silver (at 25.516 kev) the film is many times more sensitive to electromagnetic radiation, though the cadmium and other filters in the badge reduce these corrections.

The chamber has the disadvantage, compared to film, of being more fragile and easily damaged. Also pocket chambers do not give permanent records of legal value as do the filed film badge packs, but on the other hand neither do they involve periodic film replacement costs.

The advantages of the beta sensitive chamber over the commercial thick walled pocket chamber are three: first, one can read directly the total dose in a mixed beta-gamma field (as a percentage of maximum permissible exposure); second, one can determine the beta dose separately by subtracting the gamma dose determined simultaneously with the thick

walled standard chamber; and third, one can get dose measurements in a field of very low energy x-rays such as those due to internal conversion K x-rays from iron, whose energy is about 7 kev. These soft x-rays are appreciably absorbed in the wall of the standard chamber. Both chambers share the disadvantage of being accurate to only $\pm$ 10% and of leaving no permanent record. The beta chamber is not quite as rugged as the standard commercial pocket chamber, but both can stand dropping from 4 or 5 feet without damage, and in most cases without discharging the meter.

A self-reading pocket dosimeter with an optical system has a definite place in work in high radiation fields where a moment to moment check on personal dose is needed, but for wide usage it has several disadvantages. The original cost and upkeep are high, since a pocket dosimeter costs about 6 or 7 times as much as a pocket ion chamber, is more fragile, and is no more accurate. Repairs to the dosimeter necessitate returning it to the factory, with resultant time loss and expense. The self-reading pocket dosimeter as currently available commercially has a low sensitivity to most beta rays and low energy x-rays.

One manufacturer has recently marketed several beta sensitive chambers for a condenser R-meter. Of these new chambers there is one skin equivalent chamber in the range of 0 to 250 mr. It uses the same seven milligrams per square centimeter wall thickness as our pencils. This low range chamber has a volume of 170 cc and thus makes a reasonable standard chamber, but its volume and weight prevent its use as a

personnel dosimeter.

There are no commercial beta reading pocket dosimeters with which to compare our chambers. However, the soft shell Cutie Pie should have characteristics similar to the beta chamber.

The calibration system worked out for the beta pencil possesses several important features. It has the advantage of calibrating the sensitivity to beta rays against a known spectrum of radiation at a known dose rate. In other words the self absorption, air absorption, and weak sources which have constituted the principal problems with beta calibrations in the past have been eliminated by calibrating against a known spectrum of electrons in the medium. This calculation allows a plot to be made of the actual response of the instruments against the average beta energy in the solution, rather than merely giving a figure of per cent response compared to some standard for a given isotope. Thus the seven milligram wall pencil is a basic reference standard for the health physicist, whose interest is in the effective dose to the human being. Also the exposure cell described can give a more nearly absolute standard for comparison with theory, since the dose in the cavity can either be calculated, or determined by using the cavity as an ionization chamber.

The main disadvantage of the method of calibration is the contamination hazard associated with using a liquid source rather than a solid one. While the Mylar wall is extremely strong compared to the rubber hydrochloride that was tried at the start of the experiment, a 1 mg/cm^2

wall may be torn if carelessly handled. The chances of permanently contaminating the laboratory were minimized by the use of isotopes having relatively short half lives. Dangers of contamination may be further minimized by the use of radioisotopes which are distributed through a solid rather than a liquid medium.

VI. CONCLUSIONS

The electron flux spectra in dilute water solutions have been calculated for seven beta-ray emitting isotopes (Figs. 1 - 7). The average energies of these spectra and of the corresponding thin source beta-ray spectra have been determined and are given in Table II.

A laboratory standard pencil ionization chamber was built with conducting paper walls having the same 7 mg/cm^2 density as the assumed shielding over the basal layer of the human epidermis. It was therefore assumed that this chamber read correctly the physiologically important dose.

Several types of pocket ionization chambers suitable for personnel monitoring were built and calibrated. The most successful had an outer perforated wall of 24ST aluminum alloy 0.010" thick surrounding an inner ionization chamber having the same construction as the laboratory standard. All types had the same volume, geometry, and used the same type of center electrode as the Victoreen pocket chamber and hence could be read on the same Minometer.

A calibration cell was built having a central cavity with walls of 1 mg/cm^2 Mylar for calibrating the chambers with dilute water solutions of radioisotopes which emitted beta rays of various energies.

The dose rates in the cavity were determined theoretically from the measured activities in the solutions, and experimentally from the measured ionization currents to an electrode placed in the cavity. The paper walled chamber read from 10% of the calculated dose rate for S^{35} solution with an average electron energy in the solution of 52 kev, to 61% for

Y^{90} solution with average energy 694 kev. The perforated aluminum walled chamber read from about 55% of the dose rate measured by the paper walled chamber for S^{35} to 88% for Y^{90}. The drilled Al chamber thus made a suitable personnel dosimeter for beta radiation. For greater mechanical strength the aluminum wall could be made thicker with some loss of sensitivity for intermediate and high energy beta rays. Such an increase in thickness would result in a more energy independent response if the ratio of hole area to wall area were maintained and if the walls were not of such a great thickness that the "penumbra" effect would become important.

The new design pocket chambers and the Victoreen chamber were checked against a standard free air chamber and it was found that all the types of pocket chambers had practically the same response to x-rays from 20 kev to 200 kev and at 700 kev which is the effective energy of gamma rays from radium.

The reduction in the dose rate in the cavity due to its 1 mg/cm^2 walls and the large reduction due to the additional 7 mg/cm^2 wall of the paper chamber gave experimental confirmation to a conclusion drawn from the calculated electron flux curves. This conclusion was that a large part of the dose in a thick absorber irradiated with beta rays is produced by the large number of secondary electrons of very low energies which arise from the degradation of the primary spectrum.

APPENDIX

1. Sample Calculation of Electron Flux in Water Solution

The calculation of the spectrum in the medium is made according to the Spencer-Fano-Attix theory as outlined in Section II-1. A typical calculation for tungsten W^{185} is given in this section.

If the spectrum, y(T), is to be expressed as particles $cm^{-2}sec^{-1}$ $energy^{-1}$ and is to represent the flux of electrons of energy T traversing a small spherical probe per unit energy range of the spectrum, then the source must be uniform in space and constant in time. The source term, S(T), must be expressed in particles $cm^{-3}sec^{-1}$. The spectral density of electrons in the medium (particles $cm^{-3}sec^{-1}$) is given by y(T)v, where v is the velocity corresponding to T. Equation 6 of Section II-1 may be written,

$$y(T) = \left[S_Z(T)\right]^{-1} \left\{S(T) + \int_{2T}^{T} dT' \; H(T) \left[\frac{1}{T} - \frac{1}{T' - T} + \ldots\right] \quad y(T')\right\} \tag{27}$$

where H(T) is defined by

$$H(T) = 2\pi N_o r_o^{\,2} \, (Z/A) \, \beta^{-2} \tag{28}$$

where N_o is Avogadro's number; r_o the classical electron radius, and A and Z the atomic weight and number respectively. S(T) is defined by

$$S(T) = \int_{T}^{T_o} N(T')dT' \quad . \tag{29}$$

Now by defining a function $R(T) = H(T)\ y(T)$, we may rewrite Eq. (27) as

$$R(T)/H(T) = \left[S_Z(T)\right]^{-1} \left\{S(T) + \int_{2T}^{T_o} \left(\frac{1}{T} + \frac{1}{T - T'}\right) R(T')dT'\right\} . \tag{30}$$

Next, the stopping power may be expressed as the product of a stopping number $B(T)$ and a function $H(T)$,

$$S_Z(T) = H(T)\ B(T) \tag{31}$$

where $B(T)$ is a pure number. Then,

$$R(T) = \left[B(T)\right]^{-1} \left\{S(T) + \int_{2T}^{T_o} \left(\frac{T'}{T} + \frac{T'}{T - T'}\right) R(T')\ dT'/T'\right\} . \tag{32}$$

A set of points, T_i, (the "mesh") must be chosen, (see column 4, Table IV) at which the integrand is to be evaluated. In these calculations, the T_i were evenly distributed on a scale of ln T, that is, according to the formula T_o, ζT_o, $\zeta^2 T_o$, etc. The interval used for all spectra shown

had a mesh, ζ, chosen so that $\zeta^3 = 1/2$ or $\zeta^n = (1/2)^{n/3}$ (see column 3, Table IV). A smaller mesh, $\zeta^5 = 1/2$, was used for an additional calculation for P^{32}, but proved to be little improvement over the rougher mesh for the purpose at hand.

It is useful to introduce logarithmic energy intervals at this point into Eq. (32). Let $\mu = \ln T_o/T$; then $T = T_o e^{-\mu}$ and $T' = T_o e^{-\mu'}$; it follows that

$$d\mu' = - dT'/T' \quad \text{and} \quad (\mu')_{T'=2T} = (\ln T_o/T')_{T'=2T} = \ln T_o/2T = \mu - \ln 2$$

and

$$(\mu')_{T'=T_o} = (\ln T_o/T')_{T'=T_o} = \ln T_o/T_o = 0 \qquad (33)$$

so

$$R(\mu) = \left[B(T_o,\mu)\right]^{-1} \left\{S(T_o,\mu) + \int_0^{\mu-\ln 2} \left[e^{-(\mu'-\mu)} + \left(e^{-(\mu-\mu')}-1\right)^{-1}\right] R(\mu')d\mu'\right\}. \qquad (34)$$

The usual method of solving a Volterra type integral equation such as Eq. (34) is to approximate the integral by finite sums. Eq. (34) then

becomes

$$R_n = B_n^{-1} \left\{ S_n + \sum_{m=0}^{m=n-3} \left[e^{(n-m)\Delta\mu} + \left(e^{-(n-m)\Delta\mu} - 1 \right)^{-1} \right] C_m R_m \right\} \tag{35}$$

where S_n is the tabulated value of the integral source spectrum (see column 5, Table IV) for the W^{185} example taken from Fig. 3. The quantity $\left[e^{(n-m)\Delta\mu} + \left(e^{-(n-m)\Delta\mu} - 1 \right)^{-1} \right]$ is designated as K_e and is shown in column 10 of Table IV for various values of $e = n-m$. Because m is always less than n, the last term, R_m, of Eq. (35) is one of the values of R_n which has already been calculated, and C_m is a weight factor that evolves from Simpson's rule and Cote's rule.[23] For odd values of n, $C_1 = 4/9 \ln 2$, $C_2 = 2/9 \ln 2$, $C_3 = 4/9 \ln 2$, $C_4 = 2/9 \ln 2$, $C_5 = 4/9 \ln 2$, etc. For even values of n, $C_1 = 3/8 \ln 2$, $C_2 = 3/8 \ln 2$, $C_3 = 17/72 \ln 2$, $C_4 = 4/9 \ln 2$, $C_5 = 2/9 \ln 2$, $C_6 = 4/9 \ln 2$, etc. That is, Simpson's rule is used for odd values of n, and for even values of n where $m \geq 3$. Cote's rule is applied for even values of n where m = 1, 2, and 3.

Eq. (35) then becomes

$$R_n = B_n^{-1} \left\{ S_n + \sum_{m=0}^{m=n-3} K_{n-m} C_m R_m \right\} . \tag{36}$$

$$K_{n-m} = 0 \text{ for } (n-m) = 1, 2, 3 . \tag{37}$$

---

[23] See METHODS OF MATHEMATICAL PHYSICS, H. Jeffreys, B. S. Jeffreys, p. 287, Cambridge: University Press (1950).

Table IV

Calculation of Electron Flux in Water for W^{185}

(1) μ	(2) n	(3) ζ or mesh	(4) Energy W^{185}; $T_o = .428$ T(Mev)	(5) Integrated Spectrum (Fig.27) S_n	(6) See Fig. 25 H_n^{-1}	(7) Stopping Power (Fig. 26) $(S_Z)_n$	(8) $B_n = (S_Z)_n/H_n$ B_n	(9) Inverse Stopping No. $1/B_n$	(10) K_e	(11) A_n	(12) R_n	(13) $y(T)$
$\Delta\mu = 1/3 \ln 2$		$(1/2)^{n/3}$										
0	0	1.00000	.428	.000	4.23	4.20	17.77	.056	0	0	0	0
1/3 ln2	1	.79370	.3397	.018	3.85	4.49	17.30	.058	0	0	.0010	.0021
2/3 ln2	2	.62996	.2696	.085	3.44	4.88	16.78	.059	0	0	.0051	.0097
3/3 ln2	3	.50000	.2140	.195	3.02	5.38	16.27	.0617	0	0	.0120	.0202
4/3 ln2	4	.39685	.1696	.321	2.52	6.05	15.25	.0656	0.8619	0	.0209	.0293
5/3 ln2	5	.31498	.1348	.445	2.25	6.90	15.53	.0644	1.7150	.00026	.0289	.0361
2 ln2	6	.25000	.1070	.561	1.91	7.93	15.14	.0661	2.6667	.00159	.0372	.0394
7/3 ln2	7	.19843	.0849	.667	1.60	9.20	14.74	.0678	3.7922	.00414	.0455	.0405
8/3 ln2	8	.15749	.0674	.752	1.33	10.08	13.43	.0744	5.1627	.01344	.0561	.0415
3 ln2	9	.12500	.0535	.821	1.10	12.70	13.95	.0717	6.8572	.02762	.0622	.0379
10/3 ln2	10	.09922	.0427	.870	.88	14.90	13.25	.0756	8.9693	.04627	.0693	.0342
11/3 ln2	11	.07874	.0337	.907	.72	17.70	12.71	.0789	11.6139	.08510	.0783	.0312
4 ln2	12	.06250	.0268	.930	.581	21.00	12.20	.0817	14.934	.1360	.0871	.0281
13/3 ln2	13	.04961	.0212	.947	.468	25.10	11.75	.0850	19.107	.2054	.0980	.0255
14/3 ln2	14	.03937	.0168	.960	.378	30.00	11.34	.0883	24.358	.3025	.1115	.0234
5 ln2	15	.03125	.0134	.969	.301	36.00	10.82	.0922	30.968	.4300	.1290	.0215
16/3 ln2	16	.02480	.0106	.977	.241	43.50	10.49	.0956	39.220	.6030	.1510	.0202
17/3 ln2	17	.01969	.0084	.982	.193	52.00	10.01	.1000	49.519	.8253	.1807	.0193
6 ln2	18	.01563	.0067	.987	.157	62.00	9.70	.1033	63.000	1.0244	.2087	.0181

The calculation is started from a knowledge of R_o through R_4. We know that $R_o = 0$ since $S_o = 0$. $R_1 = S_1B_1^{-1}$; $R_2 = S_2B_2^{-1}$; $R_3 = S_3B_3^{-1}$; and $R_4 = S_4B_4^{-1}$. These are special cases of Eq. (27) above, since for $e = 1, 2, 3$, $K_e = 0$, and when $n = 4$, $K_4 (= 0.8619)$ is multiplied by R_o which is zero. From these values of R_n we may obtain R_5. We see from Eq. (36) that R_5 is

$$R_5 = B_5^{-1} \left\{ S_5 + \sum_{m=0}^{m=5-3} K_{5-m} \, C_m \, R_m \right\} . \tag{38}$$

Hence

$$R_5 = B_5^{-1} \left\{ S_5 + \left[C_oR_oK_5 + C_1R_1K_4 + C_2R_2K_3 \right] \right\} \tag{39}$$

and for R_6 we get by the same method,

$$R_6 = B_6^{-1} \left\{ S_6 + \sum_{m=0}^{m=6-3} K_{6-m} \, C_m \, R_m \right\} \tag{40}$$

$$R_6 = B_6^{-1} \left\{ S_6 + \left[K_6C_oR_o + K_5C_1R_1 + K_4C_2R_2 + K_3C_3R_3 \right] \right\} \tag{41}$$

$$R_7 = B_7^{-1} \left\{ S_7 + \left[K_7C_oR_o + K_6C_1R_1 + K_5C_2R_2 + K_4C_3R_3 + K_3C_4R_4 \right] \right\} . \tag{42}$$

The quantity in the square brackets, $\left[\ \right]$, is defined as A_n and is tabulated in column 11, Table IV. In terms of A_n, Eq. (36) may be written

$$R_n = B_n^{-1}\left[S_n + A_n\right] \tag{43}$$

To simply the calculation, graphs, shown in Figs. 25, 26, and 27, were made— Fig. 25 of $H(T)^{-1}$, Fig. 26 of the stopping power $S_Z(T)$, and one like Fig. 27 of the integrated beta spectrum for each isotope. The stopping power was calculated from Bethe's exact solution of Moller's relativistic electron-electron scattering formula[24] written for the weighted sum of the stopping powers of hydrogen and oxygen per unit volume of the water medium.

$$S_Z(T) = \frac{2\pi N_o e^4}{mv^2}\ \rho \sum (Z_i f_i/A_i)\left\{\ln \frac{mv^2 T}{2(1-\beta^2)I_i^2} - (2\sqrt{1-\beta^2} - 1 + \beta^2)\ \ln 2 + 1 - \beta^2 + 1/8\ (1 - \sqrt{1-\beta^2})^2\right\} \tag{44}$$

Here f_i, Z_i and A_i are the fractional mass abundance, atomic number, and atomic weight of the ith constituent of the medium. If energies are expressed in mc^2 units and if $H(T)$ is defined as

---

[24] H. A. Bethe, HANDBUCH DER PHYSIK 24, 273 (1933).

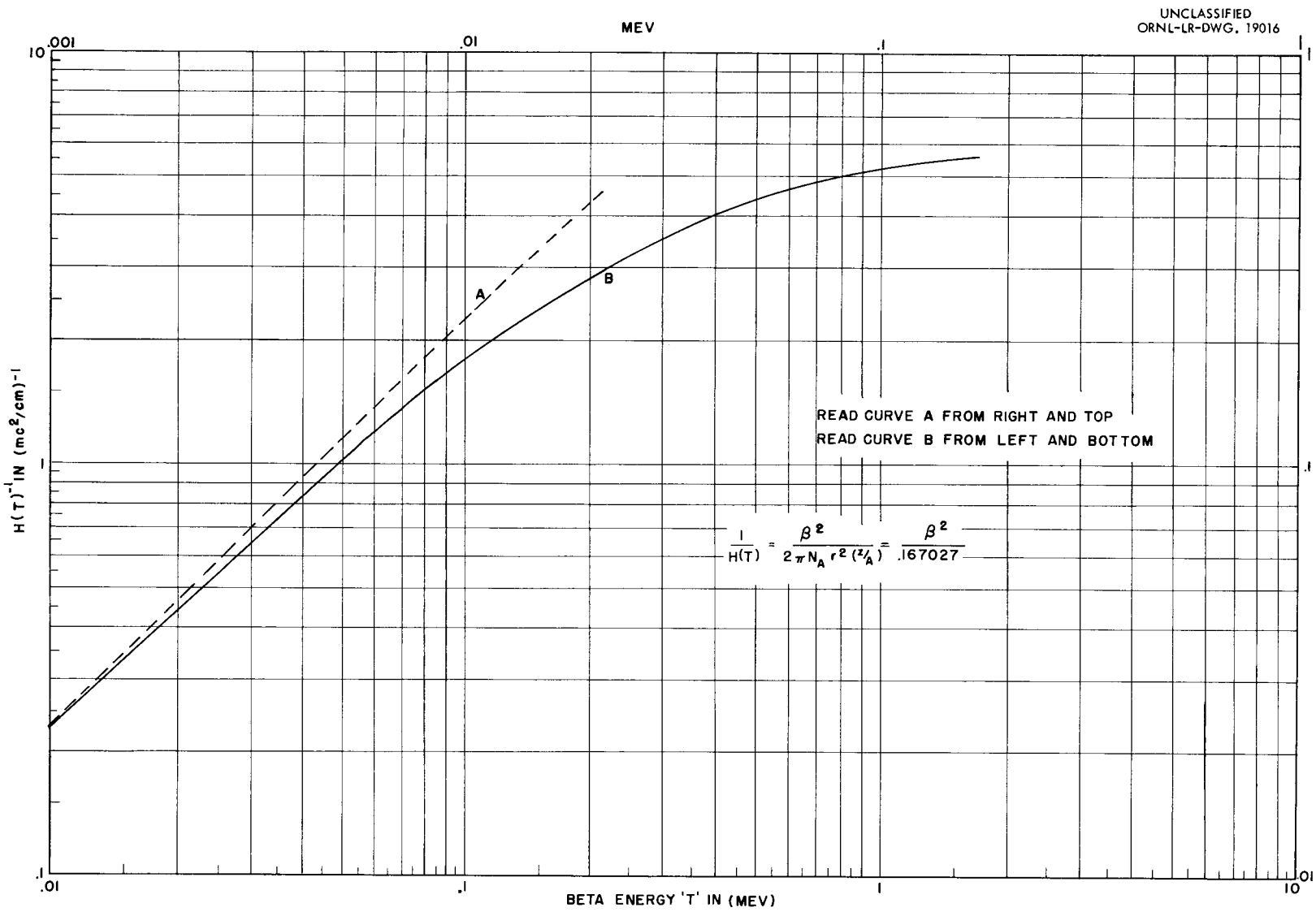
UNCLASSIFIED
ORNL-LR-DWG. 19016
MEV
.001
.01
.1
1
10
.01
.1
1
10
A
B
READ CURVE A FROM RIGHT AND TOP
READ CURVE B FROM LEFT AND BOTTOM
$\frac{1}{H(T)} = \frac{\beta^2}{2\pi N_A r^2 (Z/A)} = \frac{\beta^2}{.167027}$
$H(T)^{-1}$ IN $(mc^2/cm)^{-1}$
BETA ENERGY 'T' IN (MEV)

FIG. 25 - H (T)

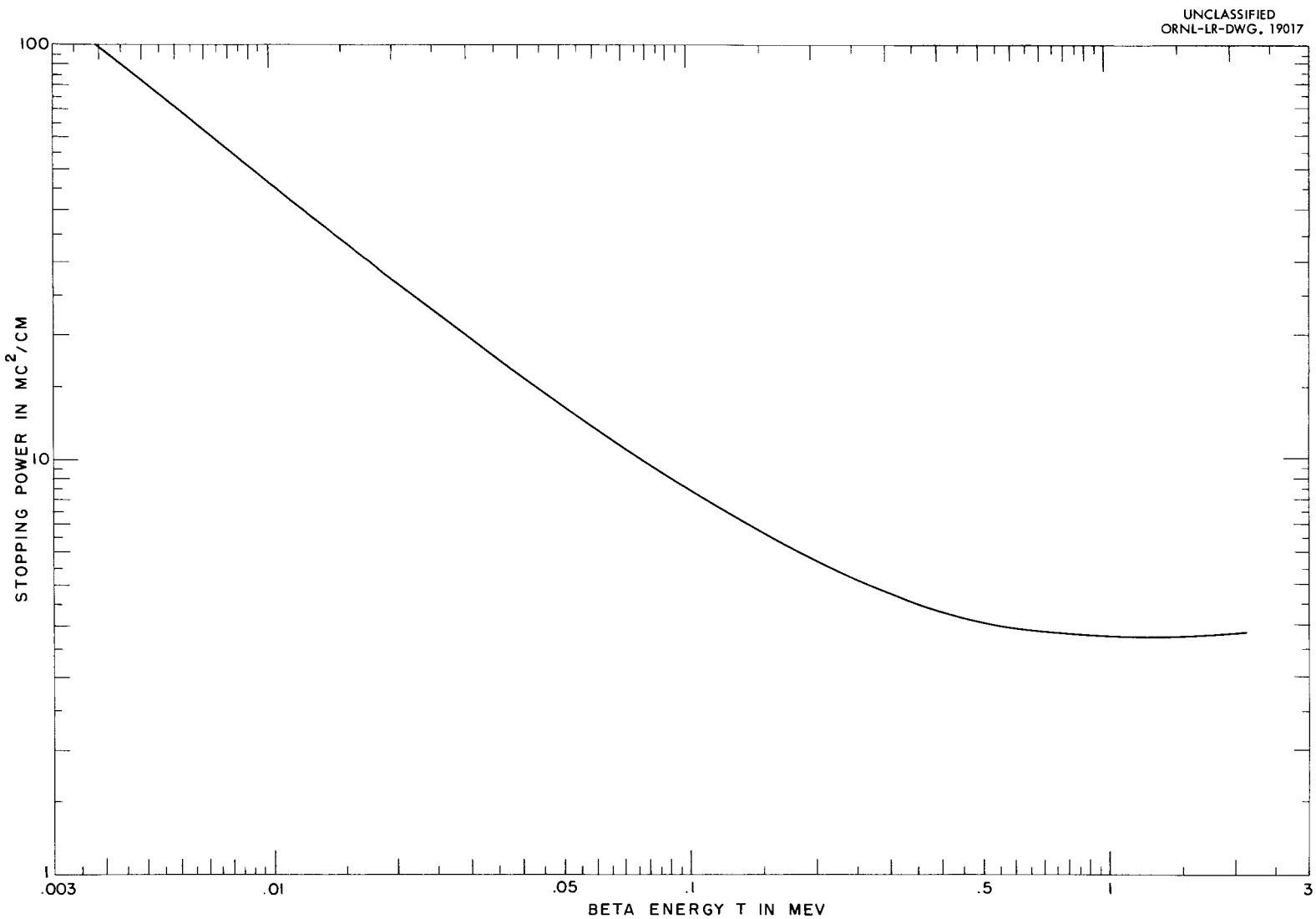

FIG. 26 - STOPPING POWER IN WATER $S_Z(T)$

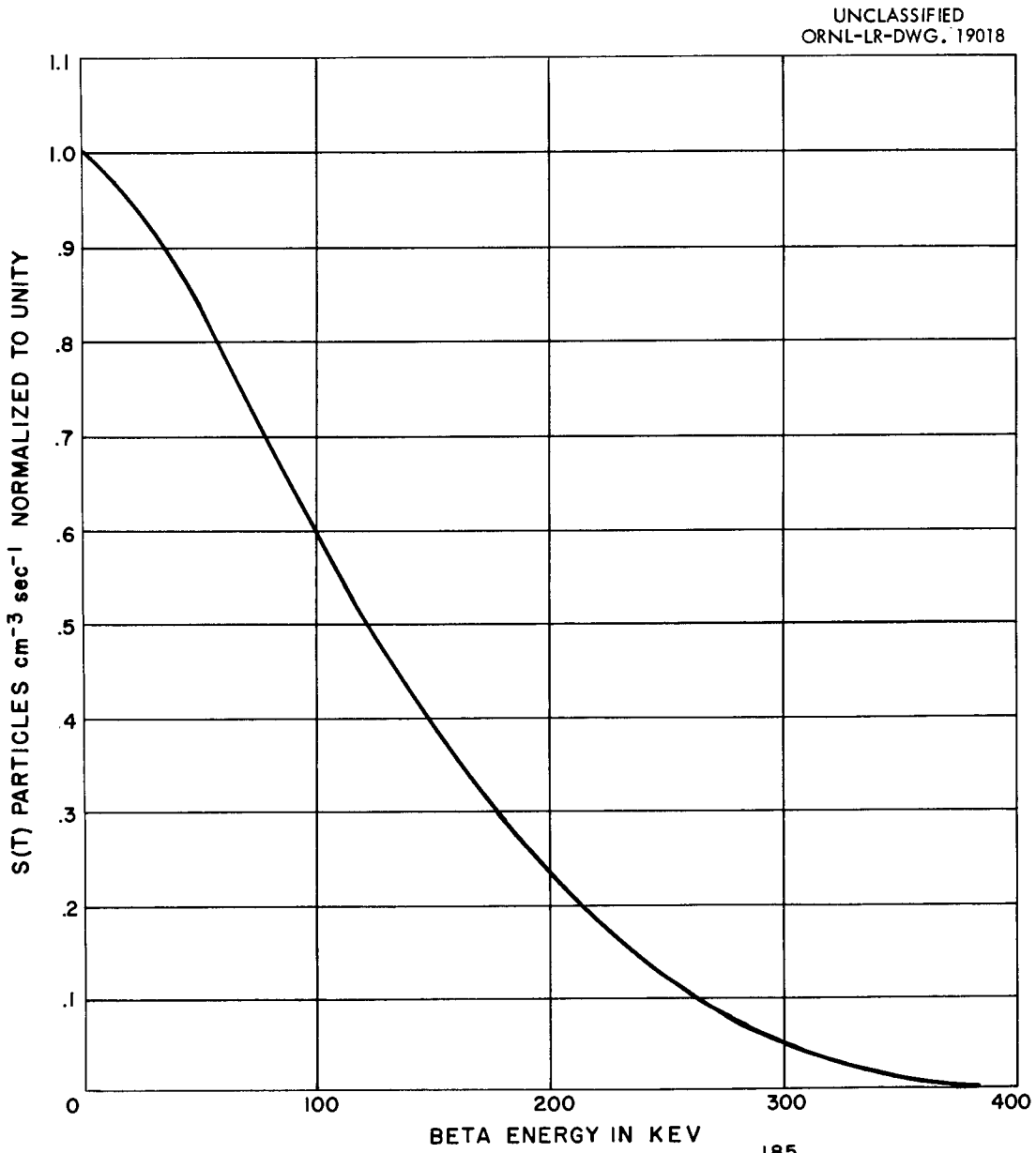

FIG. 27-INTEGRATED SPECTRUM OF W^{185}

$$H(T) = \frac{2\pi N_e r_o^{\,2}}{\beta^2} \qquad (45)$$

where N_e is the electron density of the medium and r_o is the classical electron radius, Eq. (44) becomes

$$S_Z(T) = H(T) \left\{ \ln\left[\left(\beta^2(1 - \sqrt{1-\beta^2})\right) \Big/ \left(1-\beta^2\right)^{3/2}\right] - (2\sqrt{1-\beta^2} - 1+\beta^2)\ln 2 \right.$$

$$\left. + 1-\beta^2 + 1/8\,(1 - \sqrt{1-\beta^2})^2 + \left[\sum\left((Z_i f_i)/A_i\right) \ln\left(1/(2I_i^2)\right) \Big/ \sum\left((Z_i f_i)/A_i\right)\right]\right\}. \qquad (46)$$

For water $H(T) = (0.167/\beta^2)$ and the last term in Eq. (46) has the value 17.0.

For the case of W^{185} the original beta spectrum was obtained from experimental data given in the literature.[25] P^{32}, S^{35}, and Ca^{45} are Fermi allowed and their spectral shapes were obtained from an article by Marshall.[26] There were two spectra which are first forbidden with a spin change of $\Delta I = 2$. These two, Y^{90} and Tl^{204}, have the "alpha" spectrum shape factor which can also be obtained from the Marshall

---

[25] B. Schull, "Beta Ray Spectrum of Europium and Tungsten," Phys. Rev. 74, 917 (1948).

[26] John H. Marshall, "How to Figure Shapes of Beta Ray Spectra," Nucleonics 13, No. 8 (1955).

article. The Ag^{111} is a first forbidden spectrum[27] with $\Delta I = 0, 1$ but it still has the "simple" shape[28] and thus could be obtained from the Marshall article.

In the calculation of the spectrum from W^{185}, the spectrum as given in the literature is a function, $N(H\rho)$, of the momentum, $H\rho$, in units of Gauss centimeters. The conversion of this spectrum to an energy distribution is outlined below. Since

$$N(H\rho)\, d(H\rho) = N(p)\, dp = N(T)\, dT \tag{47}$$

then

$$\left[N(p)\, dp/dT\right] dT = N(T)\, dT. \tag{48}$$

Now the kinetic energy of a beta particle is

$$T = \left(p^2c^2 + m_o^2c^4\right)^{1/2} - m_oc^2 \quad . \tag{49}$$

One may differentiate with respect to the momentum to get

$$dT/dp = \left(1/2\right)\left(2pc^2\right) \Big/ \left(p^2c^2 + m_o^2c^4\right)^{1/2} = c\left(1 + m_o^2c^2/p^2\right)^{-1/2} \tag{50}$$

---

[27] M. G. Mayer, S. A. Moskowski, and L. W. Nordheim, "Nuclear Shell Structure and Beta Decay I. Odd A Nuclei," Rev. Mod. Phys. 23, 315 (1951).

[28] A. C. Helmholz, R. W. Hayward, and C. L. McGinnis, "Radioactivities of Ag^{111}, Cd^{111}, and In^{111}," Phys. Rev. 75, 1469 (1949).

and

$$dp/dT = \left(1/c^2 + (m_o^2/p^2)\right)^{1/2}$$

$$= \left\{\left[1/(9 \times 10^{20})\right] + \left[(9.11 \times 10^{-28})^2 \Big/ \left((H\rho)^2(1.6 \times 10^{-20})^2\right)\right]\right\}^{1/2}. \tag{51}$$

By substituting Eq. (51) in (48) the energy distribution may be obtained.

2. Typical Data

A. Dose rate from assayed activity of solution

Isotope		Y^{90}, Sample II	
Max. beta energy	T_0	2.18	Mev
Av. thin source energy	$\bar{T}_N$	900	kev
Av. in water	$\bar{T}_y$	694	kev
Half life	t	64.2	hr

Original sample approximately 2.0 ml of 15.51 mc/ml at 0800 on 11-9-56, diluted with 3 ml concentrated HNO_3 and made up with water to 1 liter solution to give 0.05 N acidity.

Original assay showed $< 5 \times 10^{-4}$ mc/ml of Sr^{90} in sample, at 0.36 N HCl.

Dilute solution assayed 28.85 μc/ml ± 10% at 1210 on 11-9-56.
Dilute solution assayed 3.83 μc/ml ± 10% at 0925 on 11-17-56.

Calculated dose rate in air cavity, average corrected to 1200 on 11-9-56.

= 17.33 macre/sec = 17.33 mr/sec
(This assumes 0° C., 760 mm in cavity)

B. Dose rate from ionization in cavity (Mylar wall 1 mg/cm^2

Active length of cavity	9.1	cm
Diameter (average)	1.611	cm
Volume	18.56	cm3

Date	Time (24-hr clock)	Barometer observed mm	Temp. °C.	Observed volts across electrometer	Electrometer input resistor ohms
11-12	1046	741.1	23.1	2.076	5.30×10^{10}
	1107			2.061	5.30×10^{10}
11-14	1605	743.9	23.5	1.236	5.30×10^{10}
11-17	1510	744	23	0.0964	9.13×10^{9}
11-19	1511	749.8	22	0.0571	9.13×10^{9}

Average dose rate corrected to 1200 on 11-9-56 at NTP 16.35 mr/sec

C. Dose rate observed with pocket chambers (2. Typical Data - cont.)

1. Paper wall chambers 7 mg/cm^2

Chamber Serial Number	Date (1956)	Time 24-hr clock (hr., min.)	Exposure time (seconds)	Observed mr	mr/sec
2262	11-12	1434	31	140	
	11-14	1020	30	87	
	11-14	1044	60	170	
	11-19	1640	120	92	
4162	11-12	1438	30	137	
	11-14	1037	60	170	
	11-19	1646	120	91	
3800	11-12	1453	31	138	
	11-14	1029	60	170	
	11-19	1644	120	90	
5991	11-12	1456	30	138	
	11-14	1041	60	174	
	11-19	1630	60	46	
P.E.	11-14	1013	60	170	
	11-14	1025	60	172	
	11-19	1636	120	90	

Average dose rate corrected to 1200 on 11-9-56 at NTP 10.65

Note: The Victoreen Minometer is assumed to read correctly the dose at NTP when the chamber is at 760 mm, 22° C.

2. Drilled metal 0.010" thick surrounding paper wall chamber

Al 2S-I	11-12	1521	45	175
	11-14	1051	60	157
	11-14	1053	60	154
Al 2S-II	11-12	1524	45	178
	11-14	1056	60	153
Al 24ST-I	11-12	1527	45	178
	11-14	1058	60	150
Mg-I*	11-12	1528	45	168
	11-14	1103	60	141
	11-14	1106	60	146
Mg-II	11-12	1533	45	188
	11-14	1109	60	159

Average dose rate corrected to 1200 on 11-9-56 at NTP 9.29

* Chamber flattened so volume is probably too small.

C. Dose rate observed with pocket chambers - cont.

3. Drilled plastic 0.093" thick surrounding paper wall chamber

Chamber Serial Number	Date (1956)	Time 24-hr clock (hr., min.)	Exposure time (seconds)	Observed mr	mr/sec
4000	11-12	1535	60	173	
	11-14	1113	90	166	
6554	11-12	1537	60	169	
	11-14	1116	90	159	
7231	11-12	1541	60	170	
	11-14	1119	90	161	
9035	11-12	1543	60	161	
	11-14	1123	90	151	
Average dose rate corrected to 1200 on 11-9-56 at NTP					6.58

4. Standard Victoreen pocket chambers

623	11-12	1547	90	119	
	11-14	1208	150	124	
1067	11-12	1551	120	160	
	11-14	1210	150	124	
1513	11-12	1554	120	149	
	11-14	1213	150	116	
1723	11-12	1558	120	160	
	11-14	1215	150	124	
2260	11-12	1602	120	154	
2129	11-14	1217	150	121	
2164	11-14	1221	150	113	
Average dose rate corrected to 1200 on 11-9-56 at NTP					3.05

3. Summary of Beta Dosimeter Data

Isotope	$\bar{T}_N$ Aver. Thin Source Energy	$\bar{T}_V$ Aver. Electron Energy in Water	Assay Calc. Dose Rate	Mylar Dose Rate	Paper Dose Rate	Al-Mg Dose Rate	Standard Victoreen Dose Rate	Drilled Plastic Dose Rate
	kev		mr/sec corrected for decay, etc.					
S^{35}	55	52	0.501	N.G.*	0.0477	0.0317	0	0.0108
Ca^{45}	80	79	0.556	0.350	0.0820	0.0438	4.59×10^{-4}	0.0172
W^{185}	130	130	2.32	1.47** wop 1.67 wp	0.556	0.300	1.09×10^{-2}	0.126
Tl^{204}	243	237	2.92	2.43	1.40	0.919	4.21×10^{-3}	0.345
Ag^{111}	370	317	2.42	2.16	1.36	1.00	0.0281	0.410
P^{32} II	690	506	8.93	8.14	4.97	4.00	0.629	2.42
III	690	506	3.86	2.99	2.13	1.785	0.279	1.039
Y^{90} II	900	694	17.33	16.35	10.65	9.29	3.05	6.58

* Data bad because of plating and failure of electrometer.

** wop - without plating; wp - with plating

1. To compare dose rates calculated from W^{185} assay with Mylar wall chamber dose rates, use Mylar values extrapolated to cell filling time in order to eliminate effect of plating of isotope on Mylar.

2. To compare dose rates from W^{185} as measured in Mylar wall cavity with dose rates measured by pocket chambers, use values from cavity extrapolated to infinite time.

4. Beta Dosimeter Responses as Percentages of Various Reference Values

A. Dose rates expressed as percentages of those calculated from assay of solutions

Isotope	$\bar{T}_y$ in water	Mylar walled cavity	Paper walled chamber	Drilled Al-Mg chamber	Drilled plastic chamber	Standard Victoreen chamber
S^{35}	52	N.G.	9.5	6.3	2.2	0
Ca^{45}	79	63	14.7	7.9	3.1	0.08
W^{185}	130	64*	24	13	5.4	0.47
Tl^{204}	237	83	48	31	11.8	0.14
Ag^{111}	317	89	56	41	17	1.1
P^{32}av	506	85	55	45	27	7.2
Y^{90}	694	94	61	54	38	17.6

B. Dose rates expressed as percentages of those measured by ionization in Mylar wall cavity

Ca^{45}	79	23	12.5	4.9	0.1
W^{185}	130	33	18	7.5	0.65
Tl^{204}	237	58	38	14	0.17
Ag^{111}	317	63	46	19	1.3
P^{32}	506	66	54	32	8.4
Y^{90}	694	65	57	40	18.6

C. Dose rates expressed as percentages of those measured by paper wall chambers

S^{35}	52	66	23	0
Ca^{45}	79	53	21	0.6
W^{185}	130	54	23	2.0
Tl^{204}	237	65	25	0.3
Ag^{111}	317	73	30	2.1
P^{32}	506	82	49	13
Y^{90}	694	88	62	29

* Plating effect deducted.

Bibliography

1. Attix, F. H., and DeLaVergne, L., "Cavity Ionization as a Function of Wall Atomic Number," (to be published).

2. Bethe, H. A., HANDBUCH DER PHYSIK 24, 273, Berlin: Julius Springer (1933).

3. Birkhoff, R. D., Hubbell, H. H., Cheka, J. S., Johnson, R. M., and Ritchie, R. H., "Electron Spectrum in a Radioactive Medium," paper read at the meeting of the American Physical Society, Washington, D. C. (1956).

4. Birkhoff, R. D., HANDBUCH DER PHYSIK 34, Berlin: Julius Springer (to be published).

5. Bragg, W., STUDIES IN RADIOACTIVITY, London: McMillan and Co. (1912).

6. Clark, R. L., "Absorbers in Film Badge," Memo to J. C. Hart, Oak Ridge National Laboratory (January 19, 1948).

7. Day, F. H., "X-Ray Calibration of Radiation Survey Meters, Pocket Chambers, and Dosimeters," Washington: Government Printing Office, National Bureau of Standards, Circular 507 (July 1951).

8. Duffield, R. B., and Langer, L. M., "Disintegrations of Sn^{121} and Sn^{123}," Phys. Rev. 76, 1272 (1949).

9. Ehrlich, M., and Fitch, S. H., "Photographic X- and Gamma-Ray Dosimetry," Nucleonics 9, No. 3, 5 (1951).

10. Gray, L. H., "Absorption of Penetrating Radiation," Proc. Roy. Soc. Lond. 122A, 647 (1929).

11. Gray, L. H., "An Ionization Method for Absolute Measurement of X-Ray Energy," Proc. Roy. Soc. Lond. 156A, 578 (1936).

12. Gray, L. H., "Ionization Produced in Air at a Given Distance from a Standard Radium Source," Brit. J. Radiol. 10, 600 (1937).

13. Gray, L. H., "The Ionization Method of Measuring Neutron Energy," Proc. Camb. Phil. Soc. 40, 72 (1944).

14. Gupton, E. D., "Recombination Losses in Pocket Chambers," Nashville: A Thesis, Vanderbilt University (March 1955).

15. Helmholz, A. C., Hayward, R. W., and McGinnis, C. L., "Radioactivities of Ag^{111}, Cd^{111}, and In^{111}," Phys. Rev. 75, 1469 (1949).

16. Jeffreys, H., and Jeffreys, B. S., "Methods of Mathematical Physics," Cambridge: University Press, 287 (1950).

17. Marshall, J. H., "How to Figure the Shapes of Beta-Ray Spectra," Nucleonics 13, No. 8, 34 (1955).

18. Mayer, M. G., Moskowski, S. A., and Nordheim, L. W., "Nuclear Shell Structure and Beta Decay I. Odd A Nuclei," Rev. Mod. Phys. 23, 315 (1951).

19. Moller, C., "Zur Theorie Des Durchgangs Schneller Elektronen Durch Materie," Annalen Der Physik 14, 531 (1932).

20. Morgan, K. Z., HEALTH PHYSICS CONTROL AND NUCLEAR RESEARCH (to be published).

21. National Bureau of Standards, Research Paper No. 56. Washington: U. S. Department of Commerce (1928).

22. National Bureau of Standards, Research Paper No. 865. Washington: Journal of Research N.B.S. 16, (1928).

23. National Bureau of Standards, "Permissible Dose from External Sources of Ionizing Radiation," Handbook 59. Washington: U. S. Department of Commerce (1954).

24. Rossi, H. H., and Ellis, R. H., "Calculation for Distributed Sources of Beta Radiation," Amer. J. Roent. and Rad. Ther. 67, 980 (1952).

25. Schweiter, G. K., and Jackson, W. M., "Radiocolloids," J. Chem. Ed. 29, 513 (1952).

26. Schull, F. B., "Beta-Ray Spectrum of Europium and Tungsten," Phys. Rev. 74, 917 (1948).

27. Spencer, L. V., and Attix, F. H., "A Theory of Cavity Ionization," Rad. Res. 3, No. 3,239 (1955).

28. Spencer, L. V., and Fano, U., "Energy Spectrum Resulting from Electron Slowing Down," Phys. Rev. 93, No. 6, 1172 (1954).

29. Taylor, L. S., and Singer, G., "Improved Form of Standard Ion Chamber," read before Radiological Society of North America, Toronto (December 1929).